



A new approach for roughness representation within urban dispersion models

F. Di Nicola^{*}, E. Brattich, S. Di Sabatino

Department of Physics and Astronomy "Augusto Righi", University of Bologna, Via Iriero 46, 40126, Bologna, BO, Italy

HIGHLIGHTS

- Novel methodology to include the aerodynamic effect of buildings and trees in an operational dispersion model.
- Evaluation of the performance of the model in different scenarios at the urban and neighborhood scale.
- The addition of detailed aerodynamic effects generally improves the performance of the dispersion model.
- The inclusion of trees improves the performance especially at high spatial resolution and for densely vegetated areas.

ARTICLE INFO

Keywords:

Green infrastructure
Air quality
Vegetation
Trees
ADMS dispersion Model

ABSTRACT

The effects of green infrastructure on pollutant concentrations are greatly variable, essentially depending on the surrounding built-up environment and on local meteorological conditions. To simulate the effects of the presence of trees at urban scale, a reliable methodology is the Computational Fluid Dynamics (CFD) approach, however it needs high calculation costs. An alternative integral dispersion model is given by provided that a suitable parameterization for vegetation is included. In this work, we have developed and demonstrated a novel methodology, based on aerodynamic parameters, to include the aerodynamic effect of trees in an operational dispersion model, the ADMS-Urban. The aerodynamic parameters were derived using the morphometric method starting from open data containing information on buildings and trees. The new roughness parameter calculation method has produced the urban spatially varying roughness (USVR) and it was evaluated in different scenarios at the urban and neighborhood scale. The numerical outputs of the simulations were compared with observations from reference air quality stations collected within an ad-hoc intensive field campaign conducted in 2017 in the city of Bologna, Italy. The results of the comparison highlight that the introduction of the aerodynamic effects of buildings lead to great improvements in the performance of the model at both spatial scales and for the different study sites considered in this study. Conversely, the inclusion of trees in the calculation produces significant improvements only when conducting studies at high spatial resolution and for densely vegetated areas.

1. Introduction

Urban areas are more susceptible to the accumulation of air pollutants owing to both the large quantity and diversity of emissions in a concentrated area and to the limited dispersion caused by the physical constraints of the urban environment (Goodsite et al., 2021). Several different emergency response systems are adopted to mitigate the problem, city and regional management plans consider longer term solutions, generally consisting of land planning strategies and adoption of policies of emission reductions. Among urban planning and management plans, urban greening has become increasingly important thanks

to the ability of green infrastructure to provide benefits for environmental, social and economic ecosystem services (European Commission, 2012; Tzoulas et al., 2007). It has become evident that urban greening can counteract different urban problems, among which urban heat island, air quality, biodiversity and citizen health (Ahern, 2007; Hamada and Ohta, 2010; Kong et al., 2014; Kong et al., 2010; Wolf, 2003). Regarding the effects of green infrastructure on pollutant concentrations, results can be greatly variable, essentially depending on the built-up environment and on the meteorological conditions (Abhijith et al., 2017). Indeed, while several authors concluded that the increase in urban greening leads to a deterioration of air quality (e.g., Buccolieri

^{*} Corresponding author.

E-mail address: francesca.dinicola2@unibo.it (F. Di Nicola).

<https://doi.org/10.1016/j.atmosenv.2022.119181>

Received 9 November 2021; Received in revised form 13 May 2022; Accepted 16 May 2022

Available online 21 May 2022

1352-2310/© 2022 The Authors. Published by Elsevier Ltd. This is an open access article under the CC BY-NC-ND license (<http://creativecommons.org/licenses/by-nc-nd/4.0/>).

et al., 2009; Di Sabatino et al., 2015; Gromke and Ruck, 2007, 2009), other studies concluded that the abatement of air pollution is a key ecosystem service provided by urban vegetation (e.g., Chen, 2017; McDonald, 2015), and is the most cited economic benefit of urban trees (Song et al., 2018).

Trees have a complex and porous structure capable of altering the air flow, resulting in less dispersion through the reduction of wind speed and boundary layer heights (Vos et al., 2013; Wania et al., 2012), or in a greater dispersion due to the increase in air turbulence and mixing (Bowker et al., 2007). Trees modify turbulence and urban ventilation, and thus air pollutant dispersion, hindering the air circulation (Ries and Eichhorn, 2001). Since the trees can consist of stems, branches, stalks and leaves or needles, air flows can penetrate into the tree canopy. From a general fluid mechanical point of view, a tree can be considered as a highly complex porous medium that causes the development of boundary layers (Gromke and Ruck, 2008). In general, the aerodynamic effect of trees is parameterized as a drag term and an energy dissipation term in the evolution equations of momentum and turbulent kinetic energy, respectively (Redon et al., 2020). Consequently, the dispersion of the emitted air pollutants is conditioned by vegetation through this disturbed wind flow. The magnitude of this perturbation depends most of all on the characteristics of the vegetation itself (e.g., size, porosity, location) (Amorim et al., 2013). In general, besides than on the impinging wind conditions, the impact of green infrastructure depends mainly on the type of vegetation used, together with its relative height and thickness, which can influence the extent of mixing and deposition of pollutants. Furthermore, the air flow and vegetation impacts are substantially different in a street canyon environment compared to an open environment like a highway (Buccolieri et al., 2009; Gromke et al., 2016, 2008; Li et al., 2016). Piringer et al., (2007) demonstrated that the atmospheric flow and the microclimate are influenced by the urban characteristics, which modify the turbulent transport, dispersion and deposition of atmospheric pollutants.

The main processes caused by the presence of trees that directly impact on air quality are: (1) the deposition of pollutants on surfaces and absorption of leaves (through stomata); (2) the aerodynamic effects altering the wind flow and consequently pollutant concentrations around trees. In general, the aerodynamic and deposition effects have been studied separately. Regional-scale modeling studies have shown a small percentage of reduction in pollutant concentrations due to tree deposition (Nowak et al., 2006; Selmi et al., 2016; Tallis et al., 2011). On the other hand, urban trees show to increase pollutant concentrations through their alteration of the roughness properties of the road canyon resulting in a modification the behavior of the wind flow (Buccolieri et al., 2011; Gromke et al., 2008; Wania et al., 2012). Only a few recent studies have attempted to integrate both aerodynamic and deposition effects of tree at the urban (Janhäll, 2015; Salmond et al., 2016) or at the canyon scale (Vos et al., 2013; Vranckx et al., 2015). Studies on different real cities concluded that the aerodynamic effect of trees prevails over deposition (Jeanjean et al., 2016, 2017; Santiago et al., 2017).

Most works on the aerodynamic effects of vegetation on urban air quality are carried out by completely reconstructing urban geometry within computational domain and solving the system of governing equations by means of Computational Fluid Dynamics (CFD) codes. In these studies, the aerodynamic effects of vegetation are parameterized by considering vegetation as a porous medium, which is shaped by the addition of a momentum term (sink) to the standard fluid flow equations (for a review, see Buccolieri et al., 2019). Currently the CFD-type approaches work on very reduced spatial and temporal scales and modeling the entire city is still quite demanding in terms of computational resources. A study on a larger scale than those normally considered focused on an area of 2×2 km to analyse the effectiveness of trees in dispersing emissions from urban road traffic (Jeanjean et al., 2015). Compared to other CFD works that use idealized buildings to model wind flow and pollution dispersion, in this case a surface model was used to obtain morphological information on buildings and trees. A simplified

CFD approach (The Quick Urban Industrial Complex (QUIC) Dispersion Modeling System) has been tested on a real vegetated urban environment to investigate the role of deciduous trees in modifying the airflow of a real neighborhood (Barbano et al., 2020). The results showed that trees substantially modify the flow circulation and intensity increasing the turbulence-field heterogeneity and enhancing the turbulence intensity at the canyon interface. The study also revealed the limited impact of vegetation compared to the impact of the building density. In an urban planning perspective, to assess the effect of a possible greening intervention in a city, it would be ideal to simulate the aerodynamic effects of vegetation also at urban scale with an operational dispersion model, easy to use and very simple to set up, with lower calculation costs than the CFD approach. As the exact geometry of vegetation is not made explicit in urban scale dispersion models (Tiwari et al., 2019), in this case, a spatially-varying input data of the domain, which consider the surface roughness of vegetation, is needed.

In the field of operational dispersion modeling, only few models include the possibility to specify a surface roughness that takes into account spatial variability. Among these, SIRANE (Soulhac et al., 2011) requires two coefficients of aerodynamic roughness, i.e. the roughness of the buildings walls (default value of 0.05 m) and the roughness of the entire neighborhood, while ADMS-Urban (Atmospheric Dispersion Modeling System (CERC, 2017)), allows to consider the roughness as a spatial average for both the dispersion site and the meteorological site, or to model the spatial variation of the surface roughness on a given modeling domain (Barnes et al., 2014). The performance improvement due to the introduction of spatially varying roughness was demonstrated by modeling the center of Birmingham in the United Kingdom (6.5 km^2), starting from aerial LIDAR and cartographic data with a resolution of 200 m (Barnes et al., 2014). A further step forward consists in a modeling approach capable of quantifying the effects of aerodynamic dispersion and vegetation deposition on the concentration of pollutants on an urban scale, using the ADMS-Urban model and a spatially variable roughness calculated on the basis of the land use of Guildford in the United Kingdom (over an area of $19 \times 26 \text{ km}$) (Tiwari and Kumar, 2020). However, this approach fails to capture the effect of urban vegetation that is not classified as public green, such as roadside trees or hedges. The inclusion of building variability in estimating surface roughness based on morphometric analyzes provides good predictions of the measured wind data (Kent et al., 2017a,b; Ratti et al., 2006). A recent method for estimating morphometric parameters from an urban digital elevation model (DEM) using an image-based technique was applied to the real case of downtown Oklahoma City (OKC) in the United States (Leo et al., 2018). The calculated aerodynamic parameters were compared with the results obtained from high resolution CFD simulations, and then used in the dispersion calculations in full scale for OKC using ADMS-Urban, highlighting that it is critical to account for finer-scale morphometric variations in such scattering models to obtain accurate concentration predictions. Furthermore, the morphometric determination of aerodynamic parameters should include information on vegetation (Kent et al., 2017a,b), and on its distribution within the computation cell (dispersed or concentrated) (Godłowska and Kaszowski, 2019).

The general purpose of this study is the presentation and validation of a novel urban spatially varying roughness mapping method using the morphometric method and a 3D building and trees open database in Bologna ($44^\circ 30' 27'' 00 \text{ N}$, $11^\circ 21' 5'' 04 \text{ E}$), a medium size city located in the Po Valley in northern Italy. The specific objectives of this work are: (i) to describe the roughness parameter calculation method for solid (buildings) and porous objects (trees), (ii) to discuss the application of the calculation method in a real case, and (iii) to evaluate different scenarios considering a different presence of vegetation at the urban and neighborhood scale. The proposed method allows to choose the spatial resolution most relevant to the objectives of the study, to select the objects to be included in the calculation and to obtain the necessary parameters starting from data available in open access for most of the

urban areas around the world. Furthermore, the method improves the aerodynamic characteristics estimation of the site under study because it considers in the calculation the single objects (buildings and trees) together with their relative shapes. Following the objectives and the rationale, the paper is structured as follows. After the introduction section, the methodology for the roughness parameter calculation for both solid and porous objects and the case studies and the different spatial scales investigated are illustrated. Finally, the results are presented and discussed comparing the concentrations of pollutants modeled with the measured data.

2. Methodology

This section illustrates the methodology to include the spatially roughness information into dispersion model. The aerodynamic parameters (length of the aerodynamic roughness (z_0), and the displacement in the zero plane (z_d)) can be easily derived from five fundamental morphometric parameters (Bitter and Hanna, 2003): the average height of the building (weighted with the planar area); the maximum height of the building; standard deviation of the building height; the density of the planar area (λ_p); and the density of the frontal area, (λ_f). The fundamental morphometric parameters can be retrieved from two main sources:

- cartographic data of the territory, e.g. occupied area and height of buildings/trees.
- LIDAR data (Light Detection and Ranging) with which it is possible to obtain two models: the Digital Terrain Model (DTM) or the Digital Surface Model (DSM). In particular, DSM refers to the Earth's surface including the objects above it: buildings, trees and other artifacts.

Currently, in the field of georeferenced data, there is a huge amount of data concerning the territory, often made available by local authorities in open data format. Typically, detailed open databases on urban buildings are available in major cities. As for vegetation, many local authorities are collecting and making available data on urban vegetation using open access platforms such as OpenStreetMap (OSM) (www.openstreetmap.org) and OpenTrees project (www.opentrees.org). In this work a detailed 3D database of buildings and trees present on the domain is used, in order to obtain aerodynamic information in high spatial resolution, including details such as trees along a road or a hedge around a lawn.

Starting from theoretical and mathematical reasoning behind the roughness parameter calculation considering both solid and porous objects, the methodology is explained step by step and it is used both considering only the buildings, and considering buildings and trees together. After that, we describe the strategy adopted for the numerical simulations, providing basic information regarding the study area, the dispersion model used, its setup and the different simulations conducted.

2.1. Roughness parameter calculation in urban area: urban spatially varying roughness map

In this work, vegetation is included using the morphometric method (MacDonald et al., 1998) to calculate the zero-plane displacement (z_d) and aerodynamic roughness length (z_0) for momentum. Macdonald, (2000) replaced the logarithmic profile inside the roughness sublayer (RSL) and derived separate relations for the wind-speed profile above and below the average height of buildings. So, in the calculation of the zero-plane displacement (z_d) and aerodynamic roughness length (z_0), z is the vertical coordinate and corresponds to the average height of the roughness-elements (buildings and trees) weighted with the planar area, calculated as:

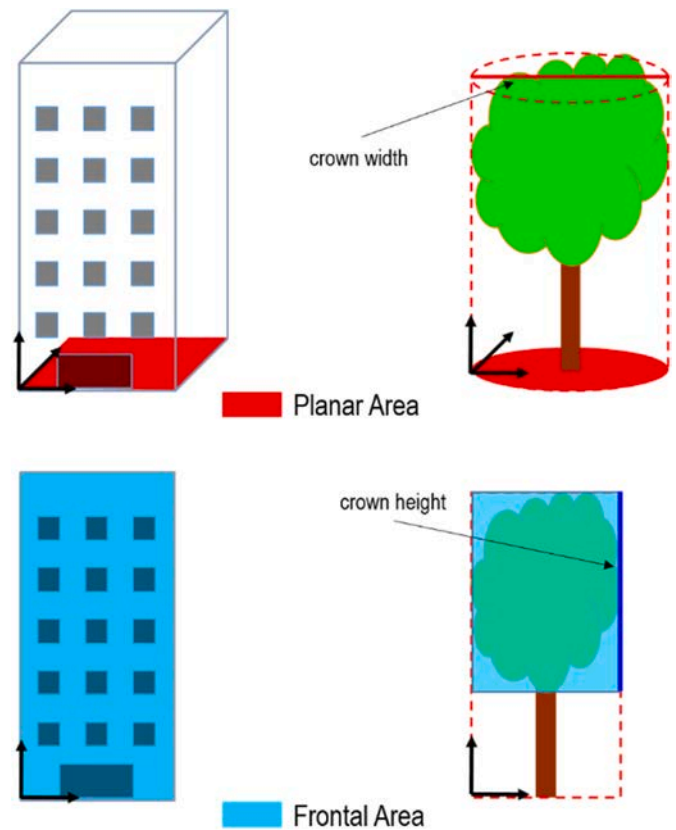


Fig. 1. Non-scaled summary diagram of morphometric parameters. Planar area (top) and front area (bottom) for buildings (left) and trees (right).

$$z = \sum \frac{A_p h}{A_p} \quad [1]$$

where A_p is the planar area of each element; h is the height of each element.

The zero-plane displacement, i.e. the height at which the mean velocity is zero due to the presence of large obstacles such as buildings/canopy, is calculated as:

$$z_d = [1 + \alpha^{-\lambda_p} (\lambda_p - 1)] \cdot z \quad [2]$$

where α is z_d correction coefficient equal to 4.43 (MacDonald et al., 1998), λ_p is the plan area index of roughness elements, z is the average height of roughness-elements. The aerodynamic roughness length (z_0), i.e. the height at which the mean velocity is zero due to substrate roughness, is calculated as

$$z_0 = \left(\left(1 - \frac{z_d}{z} \right) \exp \left[- \left(\frac{1}{\kappa^2} 0.5 \beta C_D \left(1 - \frac{z_d}{z} \right) \lambda_f \right)^{-0.5} \right] \right) \cdot z \quad [3]$$

where κ is von Karman's constant equal to 0.4 (Hogstrom, 1996), β is the drag correction coefficient set equal to 0.55 (MacDonald et al., 1998), C_D is the drag coefficient equal to 1.2, λ_f is the frontal area index of roughness elements of both solid and porous elements. This method can be further developed by including porous bodies such as vegetation (Kent et al., 2017a). The porosity of the body is considered in the calculation of λ_f :

$$\lambda_f = \frac{\{A_{fb} + A_{ft}\}}{A_{Tot}} \quad [4]$$

where A_{fb} is frontal area of buildings, A_{ft} is frontal area of trees, A_{Tot} is

Table 1

Leaf Area Index (LAI) values used for evergreen and deciduous trees and shrubs (source: Breuer et al., 2003). Leaf-off refers to the cold winter period and leaf-on refers to the warm summer period.

Tree type	LAI mean	LAI leaf-off	LAI leaf-on
Evergreen tree	6.3	6.3	6.3
Deciduous tree	5.4	3.7	7.1
Evergreen shrub	6.2	6.2	6.2
Deciduous shrub	6.2	2.4	10

the total area under consideration. A descriptor of the internal structure of the tree is the volumetric/aerodynamic porosity (P) (Kent et al., 2017a,b). The leaf area index (LAI), a dimensionless index usually defined in units of $m^2 m^{-2}$ is determined as the leaf area per unit ground area, and represents a good estimator of the porosity of the tree (Yuan et al., 2017). Thus, the frontal area index of trees is calculated using LAI values:

$$\lambda_f = \frac{\{A_{fb} + (A_{ft} \cdot LAI)\}}{A_{Tot}} \quad [5]$$

where LAI is the previously mentioned Leaf Area Index.

In this work, the parameterization of the trees starts from open data containing 3D geospatial information for buildings and trees. The basic starting data are usually stored in georeferenced files (henceforth shapefile), containing the geographical coordinates (latitude and longitude) and height of each building and tree; the perimeter of the buildings and the circumference of the crown of trees. The calculation is performed in a GIS (Geographic Information System) environment, dividing the affected area into regular cells of $100 \times 100m$ and the urban spatially varying roughness (USVR) map is obtained by Equations [2]

and [3] whereas λ_f is calculated by Equation [5].

In particular, the planar area of the buildings corresponds to the area occupied by each building, while the planar area of the trees is calculated considering the projection of the crown to the surface, therefore it corresponds to the area of the circle with a radius equal to half the width of the crown (Fig. 1). The frontal area was instead calculated starting from the perimeter of the buildings and trees divided by 4 by approximating both buildings and trees to a square shape and then multiplying the value with the height of the building. For the trees the same criterion using the circumference and height of the crown was used.

2.1.1. Approximations

The shape of the trees is approximate to that of a cylinder, where the perimeter (p) and the planar area (A_{pt}) are calculated on a circumference with a radius equal to the width of the half crown, while the volume (V) is produced as the product of the planar area and the height or the crown height, for the shrubs and the trees, respectively. The data available for the trees included information on the species and on the crown diameter classes and on the height classes. Since no specific information on the LAI of each species present in the domain was available, and considering that the data on crown and height are also approximate, we proceeded with a subdivision of the tree population into 4 classes: Deciduous trees, evergreen trees, deciduous shrubs and evergreen shrubs. We used the LAI values reported in (Breuer et al., 2003) (Table 1), considering separately the cold and the warm season to take into account the different presence of tree foliage for deciduous trees. USVR values were calculated only for buildings with a minimum height of 1 m, and for trees with a minimum height of 3 m.

Based on previous works (Coccal and Belcher, 2004; Gromke and Ruck, 2008), we chose the drag coefficient (C_D) equal to 1.2 as value representative for mixed arrays of buildings and trees. C_D is proportional

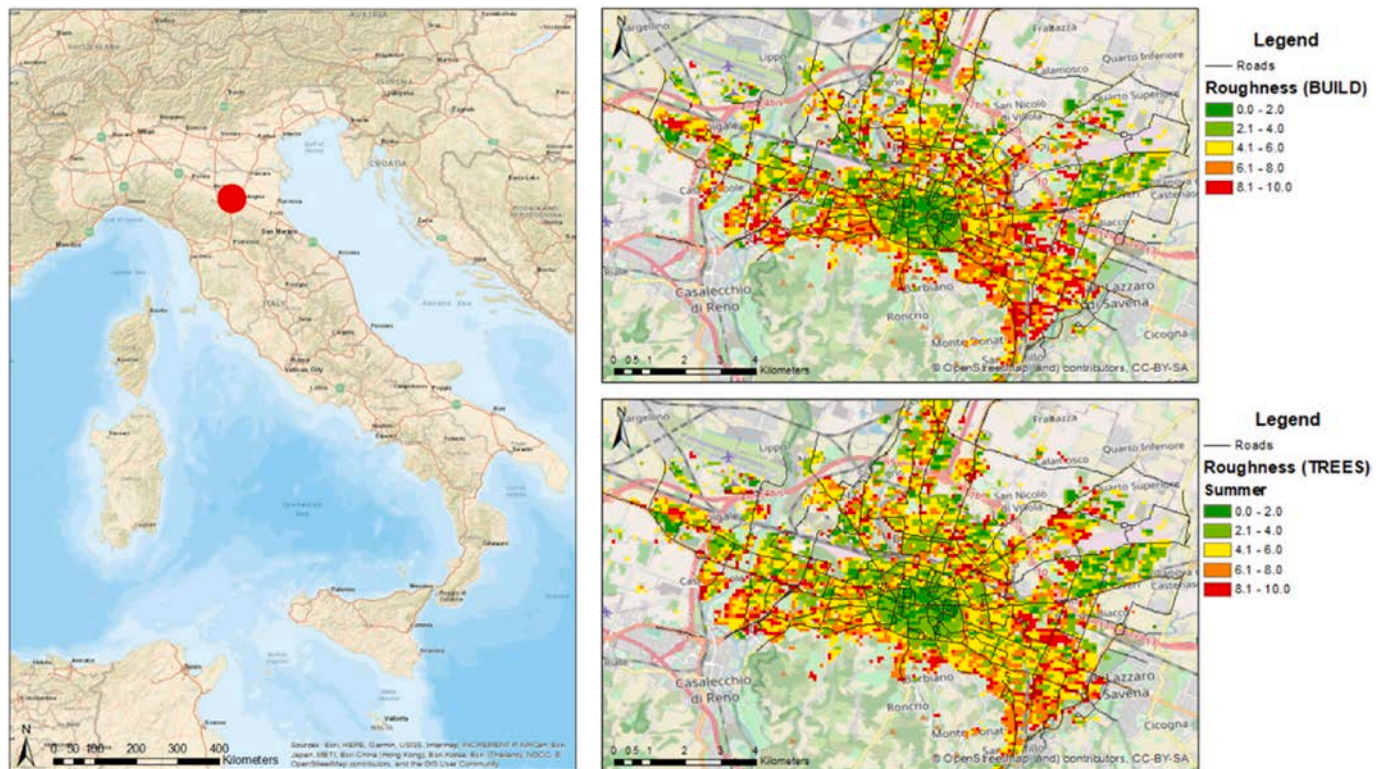


Fig. 2. Maps of Italy and of urban spatially varying roughness (USVR) for Bologna. Left) Map of Italy with Bologna position (red circle) (map source: Esri, HERE, Garmin, USGS, Intermap, INCREMENT P, NRCan, Esri Japan, METI, Esri China (Hong Kong), Esri Korea, Esri (Thailand), NGCC, OpenStreetMap and contributors, and the GIS User Community). Right) Urban spatially varying roughness (USVR) maps. Top) BUILD Roughness (BR) map, USVR calculated using only data of buildings; bottom) TREES Roughness (TRS) map, USVR calculated using data of both buildings and trees for the summer season (map source: OpenStreetMap and contributors). (For interpretation of the references to colour in this figure legend, the reader is referred to the Web version of this article.)

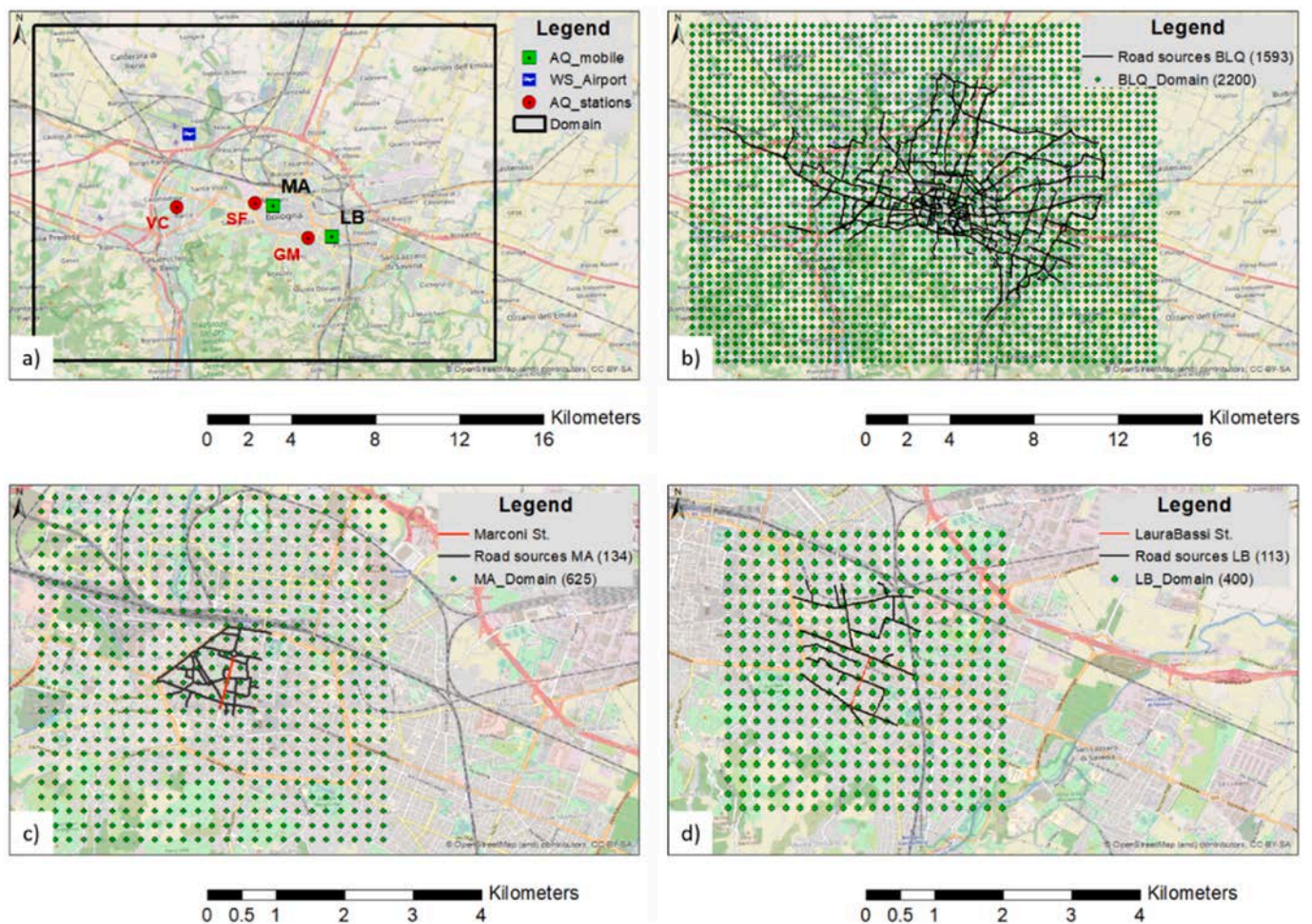


Fig. 3. Location of air quality (AQ) stations, weather stations (WS) and domain of simulations: a) Domain; AQ stations: Porta San Felice (SF), Via Chiarini (VC), Giardini Margherita (GM), and AQ mobile laboratories: Marconi (MA) and Laura Bassi (LB); b) Bologna (BLQ): 1593 links and 2200 output points; c) Marconi neighborhoods (MA): 134 links and 625 output points; and d) Laura Bassi neighborhoods (LB): 113 links and 400 output points (map source: OpenStreetMap and contributors).

to the package density. In particular, the coefficient is in the range of 0.8–1.2 for trees and for low wind velocities ($<10 \text{ m s}^{-1}$) (Gromke and Ruck, 2008), typical of the study area (see Appendix A on meteorological analysis), while for buildings it is the range between 1.2 for cubes and about 2.8 for tall cuboids for (Coccal and Belcher, 2004).

2.1.2. Steps of methodology

The methodology for including spatial roughness information in a dispersion model is practically to create roughness maps. The roughness maps are created for two different cases: the BUILD case which considers only buildings in the roughness calculation and the TREES case which considers both buildings and trees in the calculation. In particular, the creation of TREES Roughness maps is subdivided in four main steps:

1. Collection of information on trees: geometric information and information on the type of tree based on the leaves, the shape of the crown, the genus, and the species. Here the available information concerns the species of each tree.
2. Cataloging trees based on the information on trees and LAI values available. In this case the cataloging is based on 4 categories specified later.
3. Calculation of the geometric data of the trees - the variables (λ_p , λ_f , z and z_d) are calculated in a GIS (Geographic Information System) environment.

4. Roughness calculation for both trees and buildings - the variable z_0 is calculated according to the morphometric method described above and including the trees. At the end of the procedure, an USVR Roughness map is produced, containing information only in cells where either buildings either trees are present, while the procedure assigns a NaN (Not a Number) value to cells where both trees and buildings are absent.

Three different maps of the USVR are created: 1) BUILD Roughness (BR): calculated using only data of buildings (Fig. 2); 2) TREES Roughness in summer (TRS): calculated using data of both buildings and trees for the summer season (Figs. 2) and 3) TREES Roughness in winter (TRW): same as case 2) but for the winter season, i.e. absence of trees foliage for deciduous trees and shrubs.

2.2. Strategy for numerical simulations

2.2.1. Study area

The urban area of Bologna, the main city of the Emilia-Romagna region in Italy, is located in the vast flat area of the Po Plain (Fig. 2). Due to the combination of high anthropogenic emissions with the frequent stagnant conditions caused by the peculiar topographical characteristics of the Po plain, surrounded on three sides by the mountain ranges of the Alps and the Apennines, this area is recognized as one of the main pollution hotspots in Europe (Pernigotti et al., 2012; Thunis

Table 2

Information on reference monitoring stations and mobile laboratories used in this work: type and measured pollutants.

Station	Type	Measurement time resolution	Pollutants
Porta San Felice (SF)	Traffic	1-h	NO _x ; NO ₂
Via Chiarini (VC)	Suburban background	1-h	NO _x ; NO ₂ ; O ₃
Giardini Margherita (GM)	Urban background	1-h	NO ₂ ; O ₃
Marconi (MA)	Roadside (mobile)	1 min	NO _x ; NO ₂ ; O ₃
Laura Bassi (LB)	Roadside (mobile)	1 min	NO _x ; NO ₂ ; O ₃

et al., 2009). Further, Bologna is one of the main Italian road nodes, heavily interested by large-scale transportation (vehicular traffic, railway and aviation), which represent the main environmental pressure over the entire metropolitan area. In addition, due to the dominant weather conditions, the morphological characteristics of the Po Valley and the transport infrastructure impact, the background concentrations of pollutants are often high (Raffaelli et al., 2020). As from a brief analysis of the weather conditions and their comparison with the climatological records reported in Appendix A, the year 2017, which was selected as the reference year for this work, represents a worst case scenario for air quality being characterized by prolonged drought and calm wind periods.

Numerical simulations are carried out at two different spatial scales, one at the urban scale considering the whole urban area and one focusing on two specific neighborhoods of the city characterized by different presence of vegetation and building packing density (Fig. 3).

Specifically, we considered: 1) Bologna (BLQ) as urban scale, output grid: 22×16 km (55x40 points), resolution 400×400 m; 2) Marconi neighborhoods (MA), output grid: 5×5 km (25x25 points), resolution 200×200 m; 3) Laura Bassi neighborhoods (LB), output grid: 4×4 km (20x20 points), resolution 200×200 m. MA e LB are two neighborhoods in the vicinity of two parallel urban street canyons (Marconi and Laura Bassi Sts.) where one intensive experimental field campaign on air quality and turbulence levels was conducted during the period August–September 2017 (Barbano et al., 2020; Di Sabatino et al., 2020) as part of the European funded H2020 “iSCAPE” (“Improving the Smart Control of Air Pollution in Europe”) project (<https://www.iscapeproject.eu/>). Within the experimental campaign, in addition to instrumentation for the measurement of meteorological and turbulence variables at high temporal resolution and at different height levels, two mobile laboratories from the Regional Environmental Protection Agency (ARPAE) for the measurement of atmospheric pollutants (NO_x, NO₂, CO, SO₂, O₃, PM₁₀ and PM_{2.5}) were located along the two parallel urban street canyons (Fig. 3). Besides the availability of experimental data for evaluation of the output of numerical simulations, the choice of the two neighborhoods was based on the different presence of vegetation and well different morphology of the two canyons: in particular, Marconi St. is a tree-free street canyon located in the city center, while Laura Bassi St. is a tree street canyon in a residential area close to the city center.

In addition, atmospheric pollutant data were complemented with those gathered from three fixed automatic monitoring stations from ARPAE in the city of Bologna (Fig. 3), equipped with automatic analyzers for the main pollutants (PM₁₀, PM_{2.5}, NO_x, NO₂, CO, O₃, Volatile Organic Compounds (VOCs) and sulfur dioxide (SO₂)). Table 2 provides an overview of the type of station and the pollutants measured at the air quality stations in Bologna and used in this work.

As regards the meteorological observations used in this work, we used data collected from an urban synoptic station (SF) of the IdroMeteoClima Service of ARPAE Emilia-Romagna (Arpae-Simc, <https://www.arpae.it/sim/>) network and those retrieved from a synoptic

station located in the outskirts of Bologna managed from the Meteorological Service of the Air Force (WS Airport, Fig. 3).

2.2.2. Dispersion model

The ADMS-Urban model is a quasi-Gaussian plume air dispersion model capable to simulate a wide range of passive and buoyant releases to the atmosphere. This model has been already extensively verified within a large number of studies and its performance has been compared with other EU and US EPA models, such as CALPUFF and AERMOD for instance (e.g., Carruthers et al., 2000; Di Sabatino et al., 2008; Stocker et al., 2012). Within the model, the dispersion calculations are driven by hourly meteorological observations of wind speed and direction, characterized through Monin-Obukhov similarity theory. The ADMS-Urban model does account for the variation of meteorological variables between source and receptor. In the most simplified case, i.e. when a difference in the roughness length between the meteorological site and the dispersion (receptor) site is introduced, the model accounts for this difference by modifying the meteorology provided as input to the dispersion model. In the presence of a complex terrain, a version of the FLOWSTAR model (Carruthers et al., 1991) is used by the ADMS model (Carruthers et al., 1994). This module treats both dispersion over hills and regions of changing surface roughness. FLOWSTAR calculates the flow and turbulence fields over complex terrain and uses them to adjust the plume height and plume spread parameters calculated by the flat terrain model. The “Complex Terrain Module” implementation of FLOWSTAR is described in the ADMS 3 Technical Specification (Carruthers et al., 2000), also in Carruthers and Hunt (1990) and Carruthers et al. (1991), in Carruthers et al. (1988) while the basis of the theory is presented in Hunt et al. (1988a,b) and Hunt, (1985). The complex terrain module applies a three-dimensional flow and turbulence field to the dispersion modelling calculations. Indeed, ADMS-urban model can consider the presence of buildings in the calculation of the aerodynamic roughness as a spatial distribution of the roughness. In this case the flow field and turbulence values used in the dispersion modelling calculations are those output from the FLOWSTAR-D (F*) model. Changes in the surface roughness can also change the vertical structure of the boundary layer, affecting both the mean wind and levels of turbulence of the dispersion. The ADMS-Urban Complex Terrain Module models these effects using the wind-flow model FLOWSTAR. This model uses linearized analytical solutions of the momentum and continuity equations, and includes the effects of stratification on the flow. The FLOWSTAR model calculates the spatial variation of flow field and turbulence parameters that drive the dispersion. In particular, the mean wind speed boundary layer profile, u , is formulated as:

$$u(z) = \frac{u^*}{k} \left[\ln \left(\frac{z + z_0}{z_0} \right) + \psi(z, z_0, L) \right]$$

where u^* is the friction velocity (m s^{-1}), k is the Von Kármán constant (~ 0.41), z_0 is the surface roughness (in meters), is a stability term and L is the Obukhov length from Monin-Obukhov similarity theory. The mean wind speed at height z is a function of surface roughness z_0 , stability through the function, and the friction velocity u^* . In this expression for the mean wind speed, used in ADMS-Urban, the local value of z_0 represents the mixing close to the surface, and is related to the building height.

The chemical transformation of pollutants within the dispersing plume is represented using the Generic Reaction Set (GRS) chemistry scheme. In ADMS-Urban, the primary NO₂/NO_x emissions fraction is assumed constant (5%) with the GRS scheme. The GRS scheme can work when background NO_x, NO₂ and O₃ data, as well as hourly sequential meteorological data including cloud cover are available. The background values are therefore adjusted in order to ensure that they are in equilibrium, assuming:

- conservation of mass for NO_x;

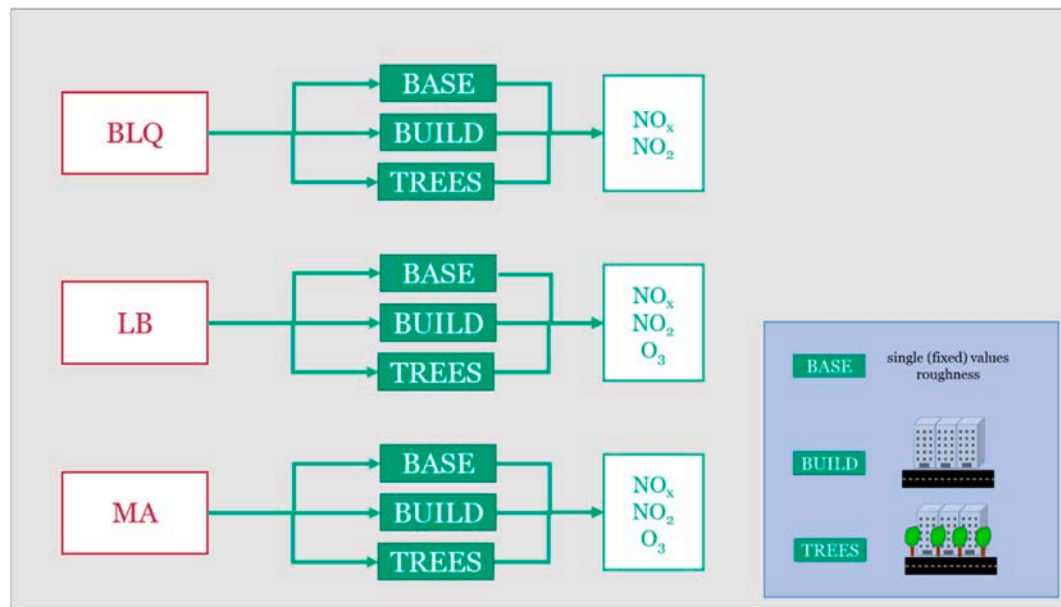


Fig. 4. Summary diagram of the simulations by scale (BLQ, LB and MA), case (BASE, BUILD and TREES) and pollutants considered (NO_x, NO₂, and O₃).

- conservation of the total mass of NO₂ and O₃;
- photo-stationary equilibrium for NO₂, NO and O₃.

2.2.3. Model setup

In order to accurately model the dispersion characteristics over a study area, the model needs as input data the topography, the meteorology, the background pollutant concentrations, the parameters of the emission sources, and the variability over time of the emissions. In Bologna, the major emission sources are traffic and domestic heating (Tositti et al., 2014), whereas no large industrial settlement is present in the surrounding area, apart from the municipal waste incinerator active in the town outskirts. Thus, a complete emission inventory describing traffic and residential heating sources in the Bologna area was created. Traffic flows in the Bologna road network were made available by the Municipality of Bologna divided into light, heavy vehicles and buses, in a georeferenced format and displayed as linear segments namely links. Given the presence of a large number of road links (about 9000), the road network for urban scale has been modeled using the number of vehicles in the stream as a discriminant (500 vehicles). Specifically, the links where the traffic flow is higher than 500 vehicles are represented explicitly as line sources, while the links with traffic flow less than 500 vehicles are combined (aggregated) over one or more grid squares. The emission inventory for the whole urban area of Bologna is constituted by 1593 road line sources represented explicitly. As for the two neighborhoods identified, and in order to correctly simulate the circulation considering the street canyons scale, it has been assumed that the emissions of all main links around the two street canyons are represented explicitly as a line source, while the emissions of all other links are combined (aggregated) over one or more grid squares. In these two cases, the emission inventory contains 134 and 113 links represented explicitly for Marconi and Laura Bassi neighborhood respectively. The diurnal and seasonal variability of emissions was considered through time varying emission factors for road and grid sources. Hourly background pollutant concentrations were obtained from suburban air quality stations of the ARPAE monitoring network (Giardini Margherita and via Chiarini in Table 2). Meteorological observations of wind speed, wind direction, surface air temperature, precipitation, solar radiation and cloud cover were obtained from the Bologna Airport synoptic weather station (WS Airport in Fig. 3; WMO number: 16140 and WMO code: LIPE), which owing to its location in the suburbs of Bologna can be considered representative of the synoptic weather impacting on the city

and not influenced by the presence of buildings in the city itself.

2.2.4. Simulations

For the purposes of this work and in order to evaluate the capability of the newly proposed method to reproduce the aerodynamic effects of trees and buildings in an operational dispersion model, dispersion modeling simulations were performed for different cases (Fig. 4), which can be summarized as follows: 1) the Base case (BASE), i.e. the base situation in which only two single roughness values at the meteorological and dispersion sites are specified; 2) Buildings case (BUILD), i.e. the case in which information of urban spatially varying roughness is added considering the presence of buildings over the simulation domain. 3) Trees case (TREES), in which information of USVR is calculated considering the presence of both buildings and trees.

Simulations were conducted both in a short-term perspective, for the verification of the methodology comparing numerical outputs with observations, and in a long-term perspective to produce concentration maps in the different cases analysed. The urban scale simulations (BLQ) cover the entire year 2017, while the neighborhood scale simulations cover the periods of the experimental campaigns, in particular spanning the period 10–23 August 2017 for Marconi (MA) and 10 August–23 September 2017 for Laura Bassi (LB).

2.2.5. Model evaluation and data analysis

Data analysis and comparison of modelling results with observations were carried out using the Model Evaluation Toolkit (CERC, 2016). In particular, the performance of the ADMS-Urban model was evaluated through the following statistical parameters: normalized mean square error (NMSE), Pearson correlation coefficient (r), fractional bias (Fb), the factor of two (Fac2). Details for the calculation of these statistical parameters are provided in Appendix B.

3. Results and discussion

In this study, we evaluated the performance of the dispersion model under different setups and scales, comparing simulated pollutant concentrations with observations from the ARPAE reference monitoring stations. In particular, we compared the numerical results obtained for three cases BASE, BUILD and TREES to evaluate the urban spatially varying roughness methodology for modelling the aerodynamic effect of trees into a dispersion model.

Table 3

Model evaluation for the simulations conducted on BASE case for urban scale (Bologna (BLQ) at Porta San Felice site (SF)) and both neighborhood scales (Marconi (MA) and Laura Bassi (LB)). Evaluation by comparison with the observations data and calculation of a set of statistical parameters (NMSE = normalized mean square error, r = Pearson correlation coefficient, Fac2 = factor of two, Fb = fractional bias, RMSE = Root mean square error ($\mu\text{g m}^{-3}$)).

Sites	Pollutant	Case	NMSE	r	Fac2	Fb	RMSE
SF	NO_x	BASE	0.1	0.9	0.9	0.3	33.7
SF	NO_2	BASE	0.1	0.8	1.0	0.1	11.4
MA	NO_x	BASE	0.8	-0.7	0.2	0.8	72.0
MA	NO_2	BASE	0.4	0.3	0.7	0.5	32.4
LB	NO_x	BASE	0.9	0.5	0.2	0.9	40.2
LB	NO_2	BASE	0.7	0.5	0.4	0.7	22.4

3.1. Model evaluation

In order to evaluate the setup of the ADMS-Urban model, hourly simulated pollutant concentrations were compared with observed values at different urban air quality stations from the regional air quality monitoring network of Emilia Romagna region (ARPAE).

Specifically, simulations conducted at city-wide scale were verified against hourly pollutant concentrations (NO_x and NO_2) observed during the year 2017 at an urban traffic air quality station located in the city center (Porta San Felice; SF in Table 2 and Fig. 3) in Bologna. Conversely, simulations conducted at neighborhood scale in the vicinity of the two urban street canyons were evaluated against data collected by mobile laboratories located along the two street canyons in Bologna (Marconi and Laura Bassi) during the previously mentioned intensive field campaign. The model evaluation carried out in the BASE case considering a single fixed value of roughness for dispersion site shows an overestimation of the model's output compared to the observations especially in neighborhood scale simulations (Table 3), as indicated by the fractional bias values. The high values of the Pearson coefficient (0.9 and 0.8 respectively for NO_x and NO_2) obtained for the urban scale simulation (BLQ) indicate the good agreement with the observations. For neighborhood scale simulations (MA and LB) the statistical parameters indicate a bad performance of the model, with low correlation coefficients. Despite this result, the numerical outputs obtained for the urban scale simulation fulfill the recommended statistical criteria for the NMSE, Fac2 and Fb parameters, specifically $\text{NMSE} \leq 1.5$, $\text{Fac2} \geq 0.5$ and $-0.3 \leq \text{Fb} \leq 0.3$ (Di Sabatino et al., 2011), Fig. 5 clearly shows the overestimation of the model especially in the maximum values.

Fig. 5 shows the time series of the simulated values at a specific point (the SF station) and cannot reflect the spatial variations in its vicinity. The reason for the consistently higher concentrations calculated in the "BASE" case with respect to the observations is due to the reduced information on the presence of obstacles in the domain provided to the model, consistently altering the dispersion of pollutants especially in the area of the city center which is dominated by the presence of tall and packed buildings. A building or other similar 3D elements can affect dispersion, deflecting the wind flow and therefore the route followed by dispersing pollutants. This deflection increases levels of turbulence, possibly enhancing dispersion thus reducing pollutant concentrations in the real case with respect to the simulated one. The ADMS-Urban model includes a relatively simple treatment of street canyons based on the Operational Street Pollution Model (OSPM), which describes the build-up of pollutants and the physics of dispersion below the urban canopy. However, only a relatively small fraction of the urban landscape can be treated by the model in this way, and in any case the module does not explicitly allow per se of the displacement of the vertical wind profile caused by the presence of obstacles (buildings and vegetation) as instead accomplished through the spatially varying roughness information. As will be shown later, the USVR approach is instead capable of accounting

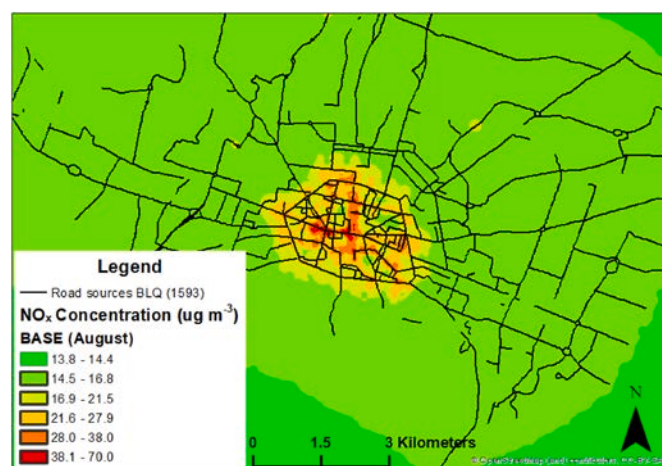


Fig. 6. Example of map of NO_x concentration in BASE cases for urban scale (BLQ), reference month: August 2017 (map source: OpenStreetMap and contributors).

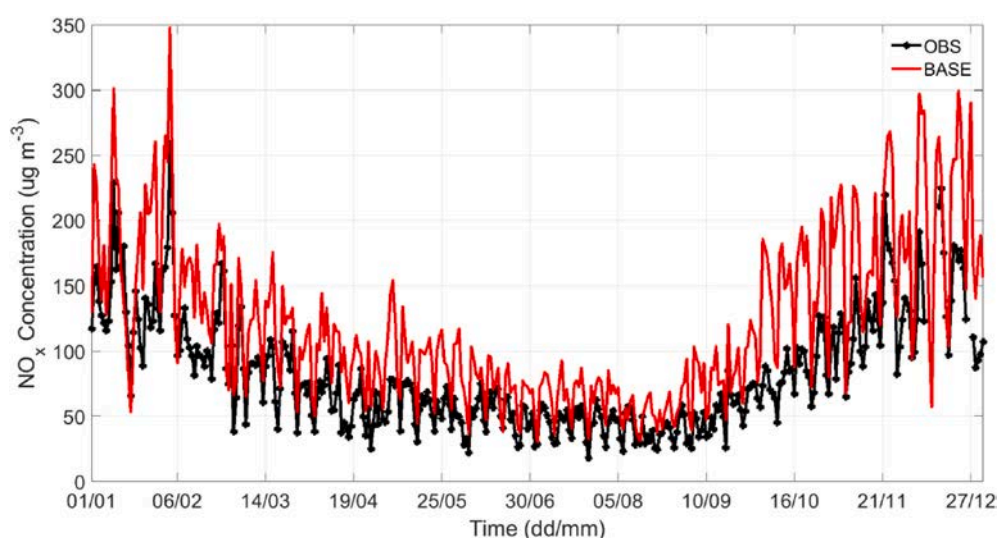


Fig. 5. Time series of NO_x daily concentration at Porta San Felice site (SF) for urban scale during 2017. Observed data in black and simulated values for BASE case in red. (For interpretation of the references to colour in this figure legend, the reader is referred to the Web version of this article.)

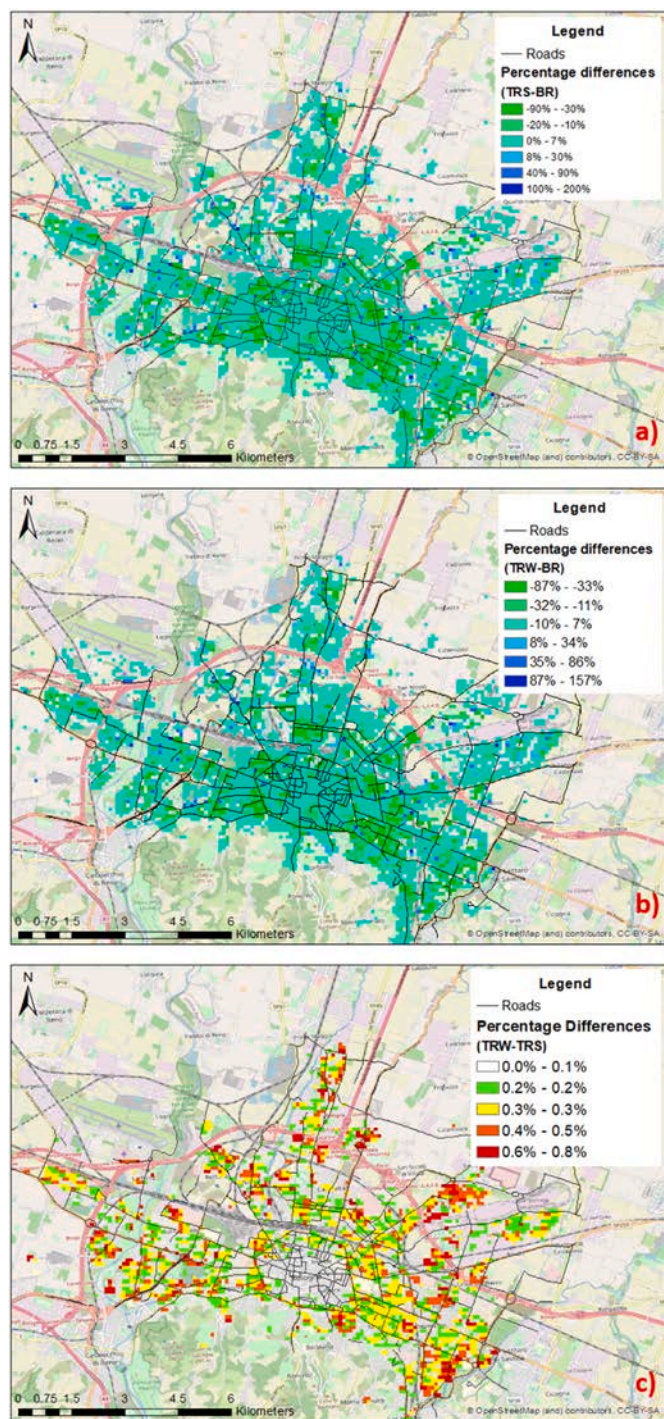


Fig. 7. Map of the percentage differences of roughness. a) between TREES roughness in summer (TRS) and BUILD roughness (BR); b) between TREES roughness in winter (TRW) and BUILD roughness (BR); between TREES roughness in winter (TRW) and TREES roughness in summer (TRS) (map source: OpenStreetMap and contributors).

for the main modifications of the wind flow, providing a better representation of aerodynamic effects caused by the presence of obstacles.

Fig. 6 shows an example of the spatial distribution of the NO_x concentration simulated by the model, in particular the average distribution for the month of August 2017.

On the map, the area with the highest NO_x concentrations coincides with the city center, and some areas with higher concentration corresponding to the busiest streets in the center can be recognized, while

lower concentrations are observed in the outskirts of Bologna. The base case results for the LB and MA sites are reported in Appendix C.

3.2. Addition of buildings and trees roughness information into dispersion simulations

The USVR method proposed in this work for the parameterization of buildings and trees has been applied for the BUILD and TREES cases, respectively with spatial roughness calculated considering only the buildings and considering both buildings and trees. The inclusion of trees in the calculation of spatial roughness on average leads to a decrease in the roughness value, due to the inclusion of trees in the calculation. Indeed, the calculation of the percentage differences between the TREES and BUILD cases shows a decrease reaching 90% (Fig. 7a) in summer, and a slightly lower reduction with a maximum value of 86.5% in winter (Fig. 7b). The seasonal effect due to the presence of foliage on deciduous trees during summer cause a difference between the roughness value in the two seasons not exceeding 1% (Fig. 7c). In particular, the percentage variations in the urban spatially varying roughness (USVR) around the air quality stations in the three sites are respectively: SF = -14% (BUILD = 5.7 m; TREES = 4.9 m); MA = -5% (BUILD = 4.2 m; TREES = 4.0 m) and LB = -39% (BUILD = 6.7 m; TREES = 4.1 m).

In computational terms, the USVR method involves an increase in the run time, a relevant aspect to take into account in the simulations planning, especially when considering the urban scale. Indeed, the time required to perform a short term run switches from 2 h to 24 min in the BASE case to 61 h and 36 min in the BUILD case for the BLQ simulations. At neighborhood scale, where the sources considered are much smaller and the simulated period is short, the required run time is far less than that needed to perform the simulation at urban scale. However, also in this case the insertion of the roughness information increases considerably the run time (1 min for the BASE case vs. 22 h and 33 min for the BUILD case).

3.2.1. Comparison between the BUILD and BASE cases

At the urban scale, the comparison of simulated and observed time series (Fig. 8a) shows the better agreement of numerical values obtained in this case with respect to the BASE case, without the tendency for the model to overestimate the maximum values. This observation is confirmed from Fig. 8b which reports the diurnal cycle for the observed and simulated concentrations in the BASE and BUILD cases, which highlights that the maximum values during the day are much closer to the observations when the information on roughness from the buildings is inserted in the simulation.

The percentage difference between the simulated concentrations in BUILD and BASE case is -24% at SF site. When considering the spatial distribution of the concentrations we observe that the percentage difference increases locally in some areas, for example it reaches -65% in the city center for the month of August (Fig. 9). Considering the minimal differences between the winter and summer, we chose to examine the results in the summer period when foliage is present on trees and when observations from the intensive experimental campaign in Bologna were available. In particular, August was chosen as the representative month for the summer period of 2017 because of its meteorological characteristics (see Appendix A) and because of the availability of the observations from the intensive field campaign in the two street canyons. The percentage differences indicate a decrease in concentration due to the aerodynamic effect of the buildings included in the model through the USVR. Furthermore, the combined effect with wind direction and speed, such as ventilation paths and stagnation areas, must be considered. Some areas of the city can be identified as turbulence producing areas, with a higher dispersion capacity and therefore lower pollutant concentrations, while other areas show an increase in concentration. In fact, the map shows precisely that there are both areas where the concentration decreases and areas where it increases, in agreement with the

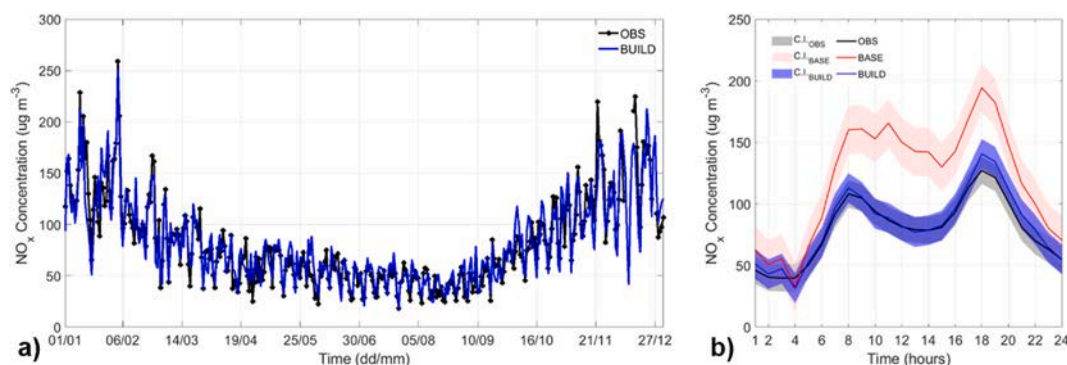


Fig. 8. NO_x daily concentration in Porta San Felice (SF) site for urban scale during 2017. Observed data in black, simulated values for Base case in red and simulated values for BUILD case in blue. a) Time series and b) Mean diurnal temporal variations, the shaded area shows the 95% confidence interval (C.I.) around the mean. (For interpretation of the references to colour in this figure legend, the reader is referred to the Web version of this article.)

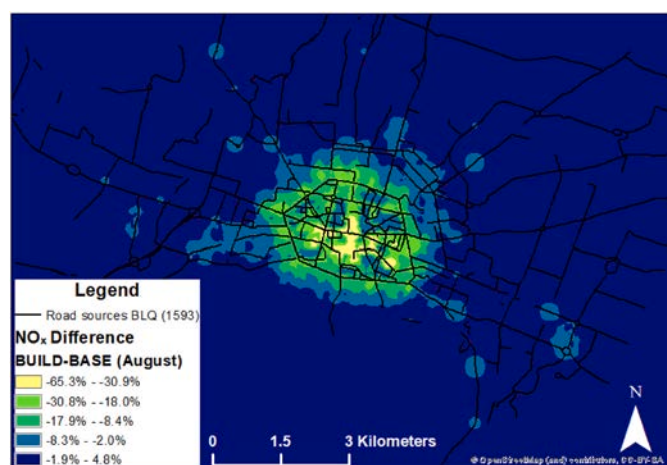


Fig. 9. Example of map of NO_x concentration difference between BUILD and BASE cases for urban scale (BLQ), reference month: August (map source: OpenStreetMap and contributors).

mass conservation law. These differences with respect to the BASE case are attributable to the USVR use that identifies roughness heterogeneity in the domain.

Even at the neighborhood scale, the comparison of the simulated and observed time series (see [Appendix C](#), Figure C 5) shows a better agreement between observations and the numerical values obtained in this case with respect to the BASE case at both neighborhoods. As the diurnal cycle for the observed and simulated concentrations in the BASE and BUILD cases also shows, the model no longer tends to overestimate, as indicated by the reduced bias between simulated and observed peak concentrations when information on the roughness of the buildings is inserted in the simulation.

For the Marconi site, the percentage difference between the simulated concentrations in the BUILD and BASE case is -69% , while the map of the percentage difference shows that in the neighborhood considered the percentage difference reaches a maximum of -60% (see [Appendix C](#), Figure C 6a). The percentage found in the MA site does not appear in the map due to the spatial average carried out at the output resolution level. Furthermore, the distribution pattern indicates that the considered area is characterized by the presence of highly packaged buildings. In Laura Bassi site, the percentage difference between the simulated concentrations in the BUILD and BASE case also is -69% , and the map of the percentage difference shows a maximum of -82% (see [Appendix C](#), Figure C 6b). In this case the spatial distribution pattern is clearly related with a different conformation of the district with low and distant buildings, as can be observed by the fact that the variation is

Table 4

NO_x statistical analysis on BUILD and TREES case for urban scale (Bologna, Porta San Felice site (SF)) and both neighborhood scales (Marconi (MA) and Laura Bassi (LB)). Analysis by comparison with the observations data and calculation of a set of statistical parameters (NMSE = normalized mean square error, r = Pearson correlation coefficient, Fac2 = factor of two, Fb = fractional bias and MB = mean bias ($\mu\text{g m}^{-3}$), RMSE = Root mean square error ($\mu\text{g m}^{-3}$)).

Sites	Pollutant	Case	NMSE	r	Fac2	Fb	MB	RMSE
SF	NO_x	BUILD	0.0	0.9	1.0	0.0	37.3	47.1
SF	NO_x	TREES	0.0	0.9	1.0	0.0	0.5	16.2
MA	NO_x	BUILD	0.1	0.7	0.9	0.1	5.5	16.4
MA	NO_x	TREES	0.1	0.7	1.0	0.1	7.3	17.0
LB	NO_x	BUILD	0.0	0.9	1.0	0.1	4.4	8.4
LB	NO_x	TREES	0.0	0.9	1.0	0.0	1.2	7.6

visible at the street level.

As previously commented, in the BASE case, the dispersion is modeled as if there were no obstacles, and is therefore guided solely by the mean wind flow. In the BUILD cases, the effect due to the presence of buildings and trees is modeled, modifying the aerodynamic properties and consequently the dispersion pattern in this case. The USVR calculation method was applied to the entire domain, divided into cells of 100×100 m. The morphological information of each single object (building and tree) present in each cell is considered in the calculation of the USVR. The high resolution calculation of the USVR provides ADMS-Urban with detailed information about each cell, allowing to calculate the local turbulence and the local variations of the mean wind field. Specifically, the NO_x concentrations simulated are more similar to those measured at street level as a result of the better representation of aerodynamic properties (see comparison of friction velocity values in [Appendix D](#)).

3.2.2. Comparison between the TREES and BUILD cases

[Table 4](#) presents the statistical parameters for the evaluation of the model performance obtained for the BUILD and TREES cases at urban and neighborhood scales for NO_x concentrations (results for other pollutants are reported in [Appendix C](#)).

The comparison of the statistical parameters obtained for the two cases does not show significant differences at urban scale (BLQ), while at neighborhood scale the performance of the model greatly improves when the aerodynamic effects of the trees are included. Specifically, for LB neighborhood with an important presence of vegetation, the mean bias between modeled and observed values decreases from 3.4 to $-0.7 \mu\text{g m}^{-3}$. The high correlation coefficients of 0.9, 0.7 and 0.9 (respectively for the urban scale, and for the two neighborhoods MA and LB simulations) indicate the good performance of the model in reproducing the observed variability of NO_x pollutant concentrations. In this case, the statistical parameters meet the previously mentioned criteria for all sites

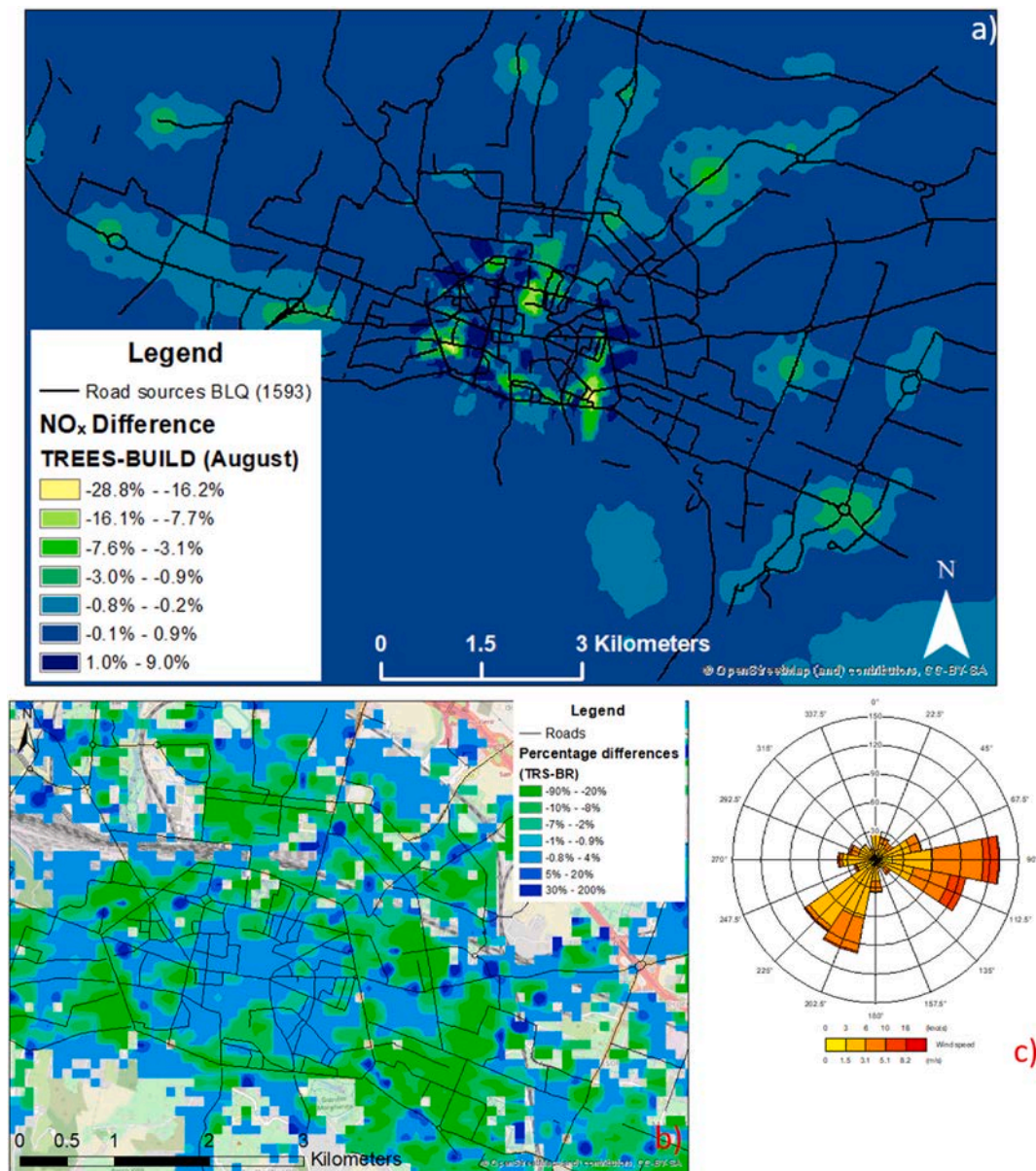


Fig. 10. Difference between TRES and BUILD cases for urban scale (BLQ): a) example of map of NO_x concentration difference; b) Map of roughness difference and c) Wind rose showing occurrences of hourly average wind direction and speed for the city of Bologna in August 2017, as recorded at the Bologna Urbana meteorological station (map source: OpenStreetMap and contributors).

and cases. The inclusion of the information of the urban spatially varying roughness improves the model's performance, as indicated by the increase in the correlation coefficients, and the decrease in Fb and MB.

In the TRES case, the improvement in the model's performance is much less evident, especially in the SF and MA sites. This can be explained from the fact that at the urban scale and for the MA neighborhood, the evaluation of the model was conducted considering only one monitoring site, located in an area of the city characterized by reduced variations in the USVR and reduced presence of vegetation. In fact, the percentage difference between the simulated concentrations in TRES and BUILD case is -1.4% in SF site for August, where the percentage variations in the USVR is only -14%. However, when considering the spatial distribution of the concentrations we observe that the percentage difference decreases in some areas, for example it reaches -29% in the city center for the month of August (Fig. 10). In fact, in Fig. 10b it can be seen that the center has areas where the concentration decreases compared to the BUILD case and others where it increases. The

areas of decrease in concentration can be identified as locations where the decrease in roughness is higher than 20%, whereas the concentrations tend to increase at intersections of busy roads and at the edges of areas of decrease.

The improvement evidenced for the simulation in the LB neighborhood is instead due to the high presence of vegetation in this area, reflected in the strong variation in roughness between BUILD and TRES (-39%). Therefore, the inclusion of trees in the roughness calculation further improves the simulation of pollutants in this case, as it better describes local aerodynamic characteristics. Fig. 11 shows the comparison of observed and simulated hourly NO_x and O₃ concentrations at the MA and LB sites considering the different simulation setups (other pollutant at neighborhood scales are reported in Appendix C together to urban scale results). The regression lines confirm the previously discussed overestimation of the model and a very low agreement of simulations with the observations at all sites obtained in the BASE case. Conversely, the agreement between simulations and observations improves considerably for the BUILD and TRES cases. Further, Fig. 11

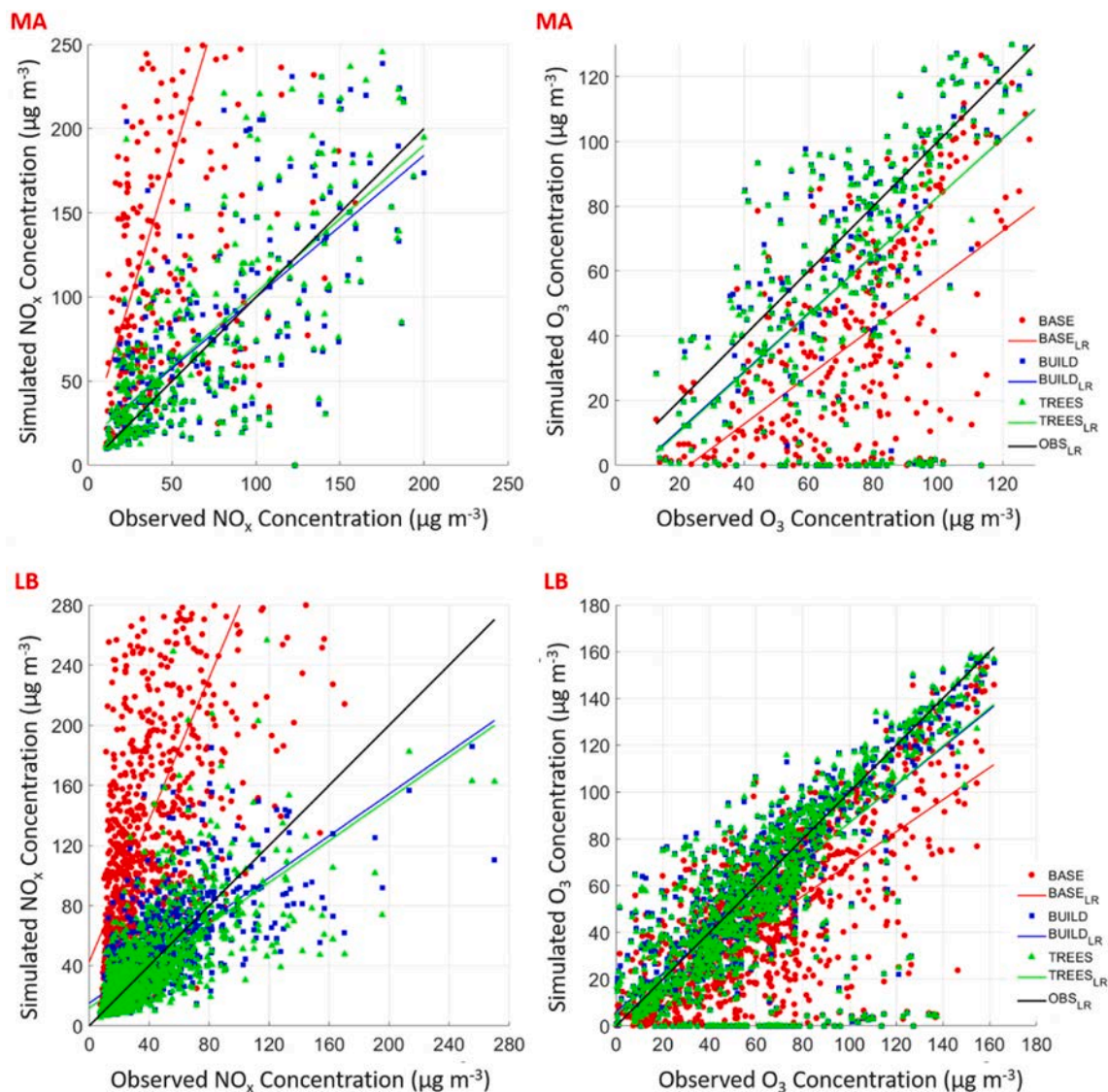


Fig. 11. Scatter plot of simulated vs. observed concentrations and linear regression lines. NO_x (left) and O₃ (right) concentration, respectively for Marconi (MA) (top) and for Laura Bassi (LB) (bottom) site.

shows that the simulations conducted with the USVR method agree better with both NO_x and O₃ observations, suggesting that the improvement in NO_x concentrations increases the capability of the model to correctly reproduce not only the share between NO and NO₂ but also all the photochemical reactions involved in the simplified chemical scheme adopted by ADMS.

It is worth to note that the USVR does not directly affect the GRS chemistry scheme implemented in ADMS-Urban, which depends on background concentrations and the presence of sunlight, air temperature of at least 18 °C, VOCs and NO_x. In fact, these parameters remain unchanged in the simulations in which USVR is used, the improvement on the estimates of NO₂ and O₃ can be indirectly attributed to the better representation of the aerodynamic properties and thus on the dispersion of pollutants. The emission data input in the model do not comprise any direct emissions of ozone, but of NO_x, which lead to ozone production and destruction by means of the simplified GRS chemistry in ADMS. So, when inserting the spatially varying surface roughness which we describe in this work leads directly to a better agreement of NO_x simulated concentrations with observations, which in turn is reflected indirectly in the improvement in ozone estimates deriving from the GRS chemical scheme.

Fig. 12 provides the evaluation of the mean NO_x and O₃ diurnal cycles, for the BUILD and TREES cases. As previously indicated by the increase in the correlation coefficients, the plots demonstrate how the model is capable to capture the diurnal cycle of NO_x concentration, that strongly reflects the pattern of source emissions, showing morning and afternoon traffic-related NO_x peaks and a dip around midday. Conversely, O₃ peaks are observed around midday, related with NO accumulation and intense solar radiation.

As from Fig. 12, NO_x diurnal cycles observed in the two urban street canyons are well different. Specifically, at Laura Bassi NO_x shows the typical traffic pattern with two peaks during the morning and evening rush hours, while at Marconi concentrations exhibit a single peak with very high concentrations in the morning rush hours gradually decreasing until reaching a nighttime minimum. This pattern, evident in observations and correctly reproduced in the simulations, is likely produced by the transits of buses, more frequent during the morning than in the evening rush hours. At both sites, the daytime O₃ cycles show a drop in correspondence of the NO_x peaks and a peak around midday. More specifically, in this case we can observe that the model tends to underestimate the O₃ peak concentrations at Laura Bassi, while at Marconi the underestimation occurs for secondary maxima observed in early

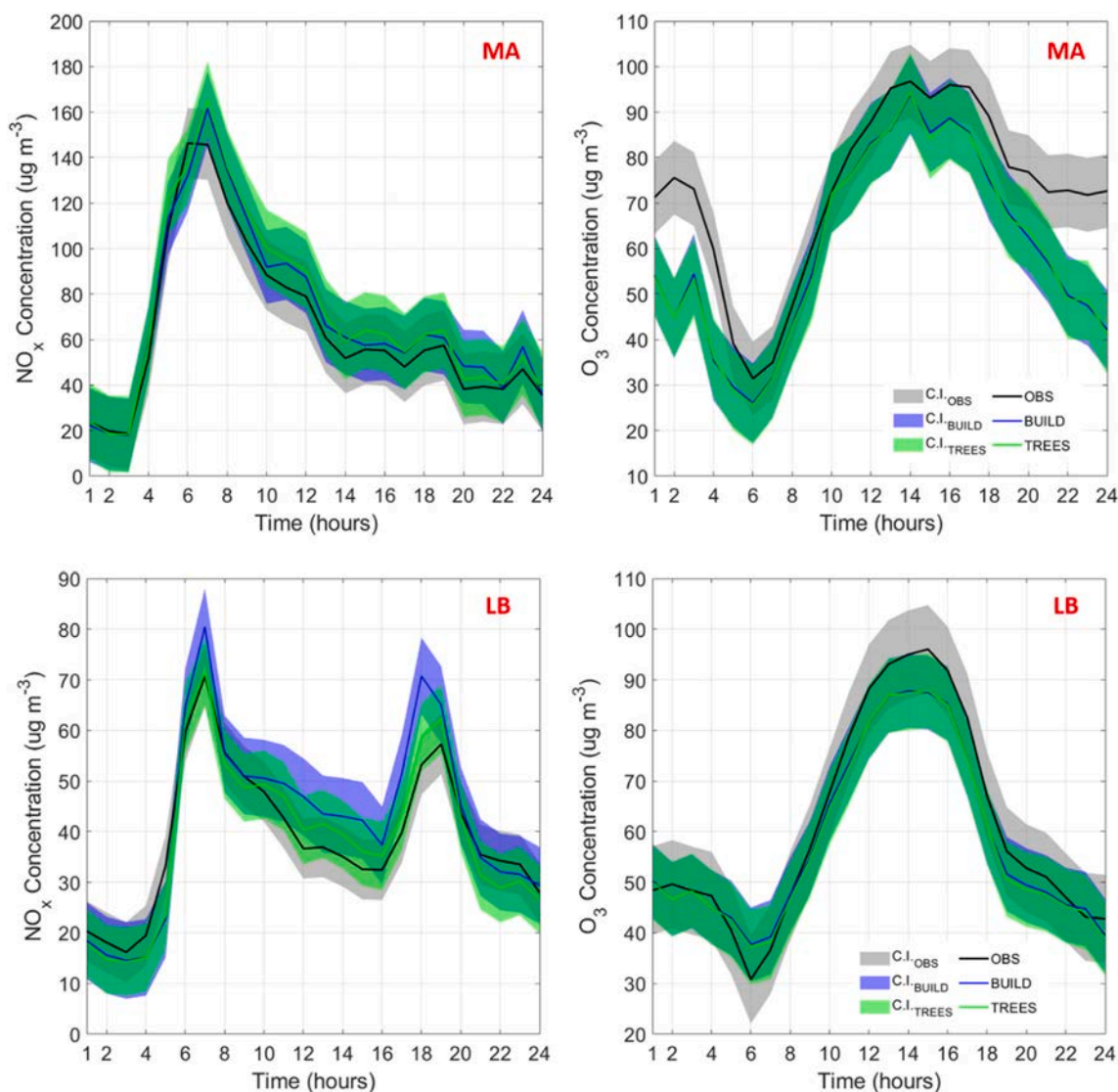


Fig. 12. Mean diurnal temporal variations of NO_x (left) and O_3 (right) concentrations, respectively for Marconi (MA) (top) and Laura Bassi (LB) (bottom) sites. The shaded area shows the 95% confidence interval around the mean.

morning and late evening. Taking into account the good model performance in reproducing NO_x concentrations, this bias in O_3 may be connected to a range of different factors, including issues with the O_3 and VOCs (Volatile Organic Compounds) background concentrations advected to the study sites and participating in the photochemical reaction cycle of ADMS, flaws in the input meteorological values of temperature and solar radiation. The results clearly suggest the presence of a relationship between the VOC/ NO_x ratio and the overestimation of the model during the hours highlighted in the diurnal cycle (see [Appendix C](#), Figure C 7), suggesting that the O_3 production tends to be more VOC-sensitive rather than NO_x sensitive (high VOC/ NO_x values) late in the evening. This is clearly linked with the biases observed in the simulated O_3 pattern, and in particular with the absence of VOCs background concentrations in our simulation setup.

The percentage difference between the simulated concentrations in TREES and BUILD case is 2.5% in MA site. Considering the spatial distribution of the concentrations we note that the percentage difference increases in some areas, reaching 9% ([Fig. 13](#)), and in other areas it shows a decrease in NO_x concentration (−2%). The concentration increase can be explained from the fact that the MA neighborhood is characterized by reduced variations in the urban spatially varying roughness (−5%) and reduced presence of vegetation.

In the TREES cases, the improvement in the model's performance is much less evident in the SF and MA sites, because the evaluation of the model was conducted considering only at one monitoring site, located at ground level in an area of the city characterized by reduced presence of vegetation and reduced variations in the USVR. The improvement highlighted for the simulation in the LB neighborhood is instead due to the higher presence of vegetation in this area. So, in this case the inclusion of trees in the roughness calculation further improves the simulation of pollutants in this case, as it better describes the local aerodynamic characteristics.

In LB site, the evaluation of the diurnal cycles shows that on average the NO_x concentrations tend to decrease in the TREES case compared to the BUILD case. In fact, the percentage difference between the simulated concentrations in TREES and BUILD case is −7.6%. Considering the spatial distribution of the concentrations we can observe that the percentage difference decreases in some areas, in particular reaching −19% within the canyon ([Fig. 14](#)), while, in the remaining area it increases of 38%. In this site, variations in the USVR due to the presence of vegetation are around −39%.

The contribution of deposition to concentration was assessed for the neighborhood scale. Simulations were conducted with the same scenarios reported in [Section 2.2](#) by adding the dry deposition to the

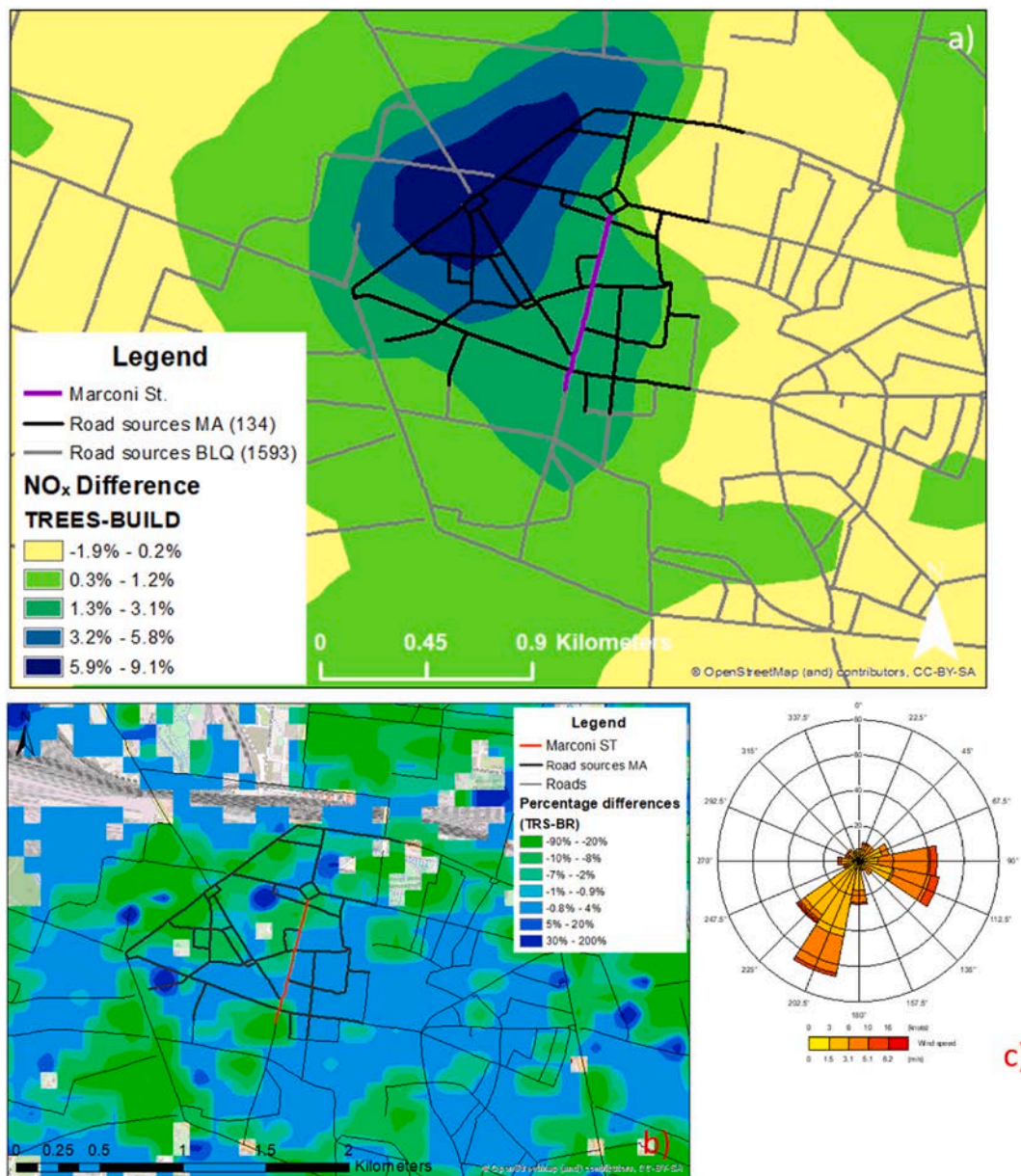


Fig. 13. Difference between TREES and BUILD cases for neighborhood scale (Marconi, MA): a) map of NO_x concentration difference; b) Map of roughness difference and c) Wind rose showing occurrences of hourly average wind direction and speed for the city of Bologna from 10 to August 23, 2017, as recorded at the Bologna Urbana meteorological station (map source: OpenStreetMap and contributors).

pollutants investigated (NO_x). The value of the deposition velocity was chosen on the basis of the type of material over which the deposition occurred: specifically, a value for urban surfaces was used in the BUILD case (0.0006 m s^{-1} (Environment Agency, 2008)), while in the TREES case, the deposition rate was calculated taking into account the surface occupied by buildings (urban surface) and trees (conifers (0.001 m s^{-1}) and deciduous (0.004 m s^{-1} (Environment Agency, 2008))).

The results indicate that deposition has a reduced impact on the concentration of gaseous pollutants such as NO_x, lowering the concentration of 0.5% at maximum in the TREES case, in agreement with previous works who suggested that the largest effects exerted by trees on pollutant concentrations are mainly related with the aerodynamic effects (Jeanjean et al., 2016, 2017; Santiago et al., 2017). Further details are available in [Appendix D](#).

4. Conclusions

This work describes a methodology to include the aerodynamic effect of buildings and trees in an operational dispersion model by the calculation of the urban spatially varying roughness, and proves not only its viability but also the improvement in the model's performance. Using the morphological method, detailed aerodynamic information of the city such as road trees otherwise not identifiable with other methodologies can be provided to the model. Using this methodology starting from georeferenced data of buildings and trees allows to choose the spatial resolution most relevant to the objectives of the study, to select the objects to be included in the calculation and to obtain data available in open access for most of the urban areas of the world. Specifically, the input elements required are open geometric data of buildings and trees and the resolution of the output is adaptable to the purpose. It is possible to refine the calculation if information regarding the species of each tree and its LAI value is available. However, this refinement may not produce

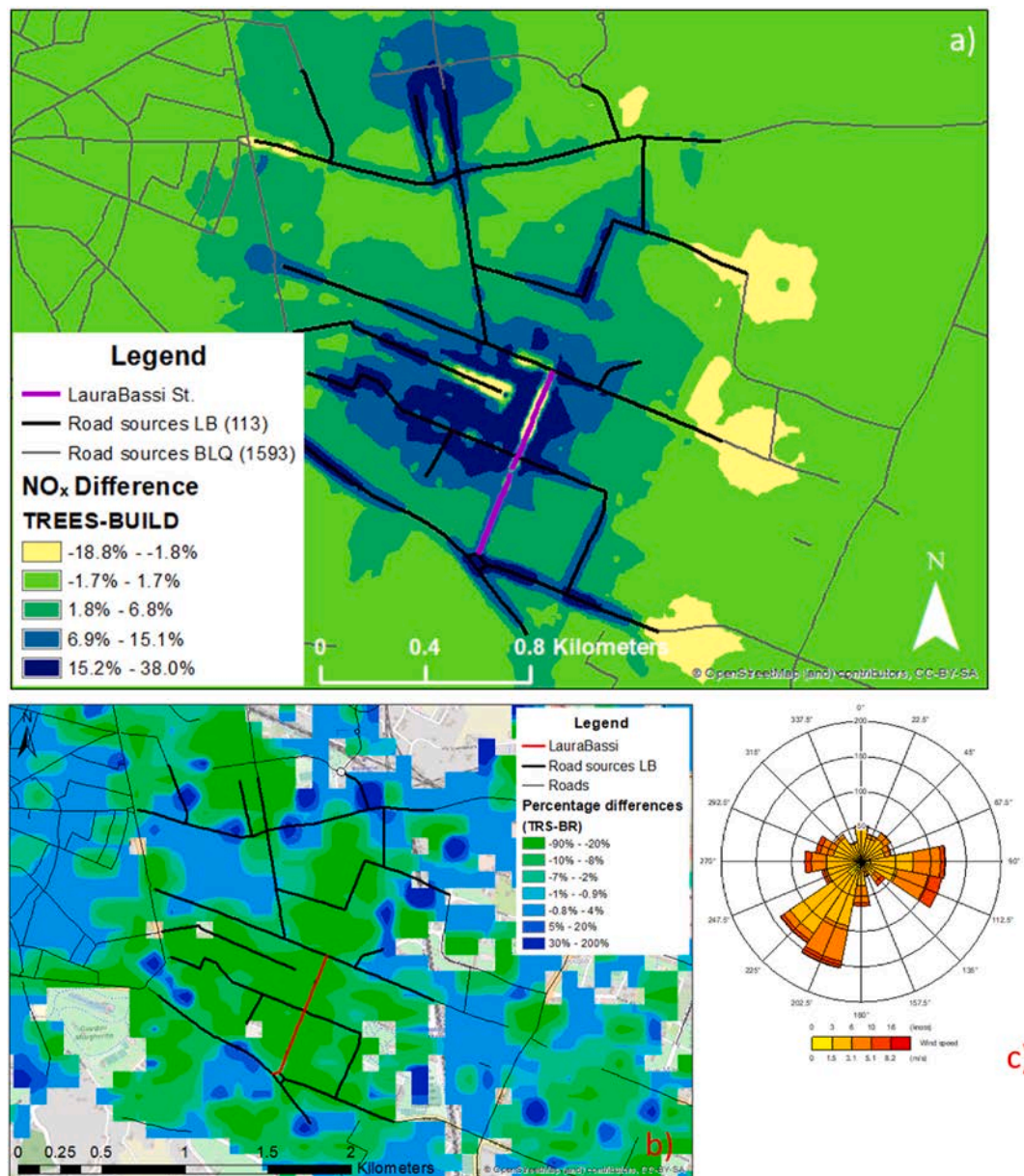


Fig. 14. Difference between TREES and BUILD cases for neighborhood scale (Laura Bassi, LB): a) map of NO_x concentration difference; b) Map of roughness difference and c) Wind rose showing occurrences of hourly average wind direction and speed for the city of Bologna from 10 to August 23, 2017, as recorded at the Bologna Urbana meteorological station (map source: OpenStreetMap and contributors).

major improvements, considering the reduced differences we obtained for Bologna between the winter and the summer periods characterized by different presence of foliage for deciduous trees.

To prove the methodology viability and the improvement in the model's performance, the three cases (BASE, BUILD and TREES) are investigated at urban (BLQ) and neighborhood scale (MA and LB), for a total nine simulation runs with the ADMS dispersion model. The model evaluations were carried out by comparison of simulated concentrations with measured data from reference air quality stations in the city and calculating performance statistical parameters indicative of correlation and bias between the simulated values and observations.

Despite the urban-scale model in the BASE case fulfills the recommended criteria for the NMSE, Fac2 and Fb parameters, it shows a tendency for the simulation to overestimate observed concentrations. Instead, the simulations conducted for the two neighborhoods show a poor model's performance. Significant improvements were obtained at all scales and sites introducing USVR. The insertion of the roughness due

to buildings and trees has produced different results based on the spatial scale and on the characteristics of the dispersion site. The improved treatment of urban roughness elements leads to a better agreement between simulated and observed pollutant concentrations, both locally in the area of reduced roughness and downwind of that area. This is because the spatially varying surface roughness better describes the presence of obstacles and the caused displacement in the wind flow. This would not be the case if introducing just a smaller value, but constant in space, for the roughness length; indeed in this case the reduced value would not be representative of the spatially varying presence of built surfaces, vegetated areas, or open road conditions and the resultant modifications in the wind flow previously described.

At the urban scale, the presence of trees does not seem to significantly alter the results. However, this observation may result from the fact that the observations used to evaluate the model performance were available only for a not densely vegetated site. Indeed, the spatial map highlights the presence of areas characterized by significant variations

in pollutant concentrations where vegetation is present. At the neighborhood scale, the inclusion of vegetation significantly improves the agreement of the simulations with observations, especially for vegetated areas such as Laura Bassi in our case. Therefore, this methodology is strongly recommended to improve the performance of dispersion simulations, and particularly to limit the overestimation of the simulated concentrations. The inclusion of vegetation is particularly necessary in high spatial resolution studies, and for densely vegetated sites. In inhomogeneous urban cases, in order to study local dispersion and the influence of vegetation, it is instead advisable to divide the area into homogeneous sub-areas.

CRediT authorship contribution statement

F. Di Nicola: Conceptualization, Methodology, Software, Writing – review & editing, Data curation, Writing – original draft, Software, Validation, Visualization, Investigation. **E. Brattich:** Conceptualization, Methodology, Software, Writing – review & editing, Data curation, Writing – original draft, Software, Validation, Visualization, Investigation. **S. Di Sabatino:** Conceptualization, Methodology, Software, Writing – review & editing, Supervision.

Declaration of competing interest

The authors declare that they have no known competing financial interests or personal relationships that could have appeared to influence the work reported in this paper.

Acknowledgments

This work has been supported by the iSCAPE (Improving the Smart Control of Air Pollution in Europe) project funded by the European Union's H2020 Research and Innovation programme (H2020-SC5-04-2015) under the Grant agreement No. 689954. The authors wish to acknowledge to Francesco Barbano and Massimo Bacchetti from the Department of Physics and Astronomy of the University of Bologna and Luca Torreggiani, Enrico Minguzzi, and Carla Barbieri from the ARPAE Regional Environmental Protection Agency and the Emilia-Romagna Region for their effort in the implementation of the experimental field campaign; ARPAE for providing the air quality data; OpenStreet Map and contributors for providing the maps.

Appendix A. Supplementary data

Supplementary data to this article can be found online at <https://doi.org/10.1016/j.atmosenv.2022.119181>.

References

- Abhijith, K.V., Kumar, P., Gallagher, J., McNabola, A., Baldauf, R., Pilla, F., Broderick, B., Di Sabatino, S., Pulvirenti, B., 2017. Air pollution abatement performances of green infrastructure in open road and built-up street canyon environments – a review. *Atmos. Environ.* 162, 71–86. <https://doi.org/10.1016/j.atmosenv.2017.05.014>.
- Ahern, J., 2007. Green infrastructure for cities: the spatial dimension. In: *Cities of the Future: towards Integrated Sustainable Water and Landscape Management*. IWA Publishing.
- Amorim, J.H., Rodrigues, V., Tavares, R., Valente, J., Borrego, C., 2013. CFD modelling of the aerodynamic effect of trees on urban air pollution dispersion. *Sci. Total Environ.* 461–462, 541–551. <https://doi.org/10.1016/j.scitotenv.2013.05.031>.
- Barbano, F., Di Sabatino, S., Stoll, R., Pardyjak, E.R., 2020. A numerical study of the impact of vegetation on mean and turbulence fields in a European-city neighbourhood. *Build. Environ.* 186, 107293 <https://doi.org/10.1016/j.buildenv.2020.107293>.
- Barnes, M.J., Brade, T.K., Mackenzie, A.R., Whyatt, J.D., Carruthers, D.J., Stocker, J., Cai, X., Hewitt, C.N., 2014. Spatially-varying surface roughness and ground-level air quality in an operational dispersion model. *Environ. Pollut.* 185, 44–51. <https://doi.org/10.1016/j.envpol.2013.09.039>.
- Bowker, G.E., Baldauf, R., Isakov, V., Khlystov, A., Petersen, W., 2007. The effects of roadside structures on the transport and dispersion of ultrafine particles from highways. *Atmos. Environ.* 41, 8128–8139. <https://doi.org/10.1016/j.atmosenv.2007.06.064>.
- Breuer, L., Eckhardt, K., Frede, H.G., 2003. Plant parameter values for models in temperate climates. *Ecol. Model.* 169, 237–293. [https://doi.org/10.1016/S0304-3800\(03\)00274-6](https://doi.org/10.1016/S0304-3800(03)00274-6).
- Britter, R.E., Hanna, S.R., 2003. Flow and dispersion in urban areas. *Annu. Rev. Fluid Mech.* 35, 469–496. <https://doi.org/10.1146/annurev.fluid.35.101101.161147>.
- Buccolieri, R., Gromke, C., Di Sabatino, S., Ruck, B., 2009. Aerodynamic effects of trees on pollutant concentration in street canyons. *Sci. Total Environ.* 407, 5247–5256. <https://doi.org/10.1016/j.scitotenv.2009.06.016>.
- Buccolieri, R., Salim, S.M., Leo, L.S., Di Sabatino, S., Chan, A., Ielpo, P., de Gennaro, G., Gromke, C., 2011. Analysis of local scale tree-atmosphere interaction on pollutant concentration in idealized street canyons and application to a real urban junction. *Atmos. Environ.* 45, 1702–1713. <https://doi.org/10.1016/j.atmosenv.2010.12.058>.
- Buccolieri, R., Santiago, J.L., Rivas, E., Sánchez, B., 2019. Reprint of: review on urban tree modelling in CFD simulations: aerodynamic, deposition and thermal effects. *Urban For. Urban Green.* 37, 56–64. <https://doi.org/10.1016/j.ufug.2018.07.004>.
- Carruthers, D.J., Edmunds, H.A., Lester, A.E., McHugh, C.A., Singles, R.J., 2000. Use and validation of ADMS-Urban in contrasting urban and industrial locations. *Int. J. Environ. Pollut.* 14, 364–374.
- Carruthers, D.J., Holroyd, R.J., Hunt, J.C.R., Weng, W.-S., Robins, A.G., Apsley, D.D., Smith, F.B., Thomson, D.J., Hudson, B.J., 1991. UK Atmospheric Dispersion Modelling System. In: van Dop, Han, Kallos, George (Eds.), *Proceedings of the 19th NATO/CMS International Technical Meeting on Air Pollution Modeling and its Application*. September 1991, Crete, Greece. Plenum Publishing Corporation, New York.
- Carruthers, D.J., Holroyd, R.J., Hunt, J.C.R., Weng, W.-S., Robins, A.G., Apsley, D.D., Thomson, D.J., Smith, F.B., 1994. UK-ADMS: a new approach to modeling dispersion in the Earth's atmospheric boundary layer. *J. Wind Eng. Ind. Aerod.* 52, 139–153. [https://doi.org/10.1016/0167-6105\(94\)90044-2](https://doi.org/10.1016/0167-6105(94)90044-2).
- Carruthers, D.J., Hunt, J.C.R., 1990. Fluid mechanics of airflow over hills: turbulence, fluxes, and waves in the boundary layer. In: Blumen, W (Ed.), *Atmospheric Processes in Complex Terrain*, 23. American Meteorological Society, Boston, MA, pp. 83–103.
- Carruthers, D.J., Hunt, J.C.R., Weng, W.-S., 1988. Computational models of air flow over hills. *Proc. Int. Conf. ENVIROSOFT*. 489–492.
- CERC, 2017. ADMS-urban Urban Air Quality Management System Version 4.1 User Guide CERC 390.
- CERC, 2016. Model Evaluation Toolkit User Guide 1–63.
- Chen, W.Y., 2017. Urban nature and urban ecosystem services. In: Tan, P.Y., Jim, C.Y. (Eds.), *Greening Cities: Forms and Functions*. Springer Singapore, Singapore, pp. 181–199. https://doi.org/10.1007/978-981-10-4113-6_9.
- Coccal, O., Belcher, S.E., 2004. A canopy model of mean winds through urban areas. *Q. J. R. Meteorol. Soc.* 130, 1349–1372. <https://doi.org/10.1256/qj.03.40>.
- Di Sabatino, S., Barbano, F., Brattich, E., 2020. The multiple-scale nature of urban heat island and its footprint on air quality in real urban environment. *Atmosphere (Basel)* 11, 1186.
- Di Sabatino, S., Buccolieri, R., Olesen, H.R., Ketzel, M., Berkowicz, R., Franke, J., Schatzmann, M., Schlünzen, K.H., Leitl, B., Britter, R., Borrego, C., Costa, A.M., Castelli, S.T., Reisin, T.G., Hellsten, A., Saloranta, J., Moussiopoulos, N., Barmas, F., Brzozowski, K., Goricsán, I., Balczó, M., Bartzis, J.G., Efthimiou, G., Santiago, J.L., Martilli, A., Piringer, M., Baumann-Stanzer, K., Hirtl, M., Baklanov, A.A., Nuterman, R.B., Starchenko, A.V., 2011. COST 732 in practice: the MUST model evaluation exercise. *Int. J. Environ. Pollut.* 44, 403–418. <https://doi.org/10.1504/IJEP.2011.038442>.
- Di Sabatino, S., Buccolieri, R., Pappacogli, G., Leo, L.S., 2015. The effects of trees on micrometeorology in a real street canyon: consequences for local air quality. *Int. J. Environ. Pollut.* 58, 100–111. <https://doi.org/10.1504/IJEP.2015.076587>.
- Di Sabatino, S., Buccolieri, R., Pulvirenti, B., Britter, R.E., 2008. Flow and pollutant dispersion in street canyons using FLUENT and ADMS-Urban. *Environ. Model. Assess.* 13, 369–381. <https://doi.org/10.1007/s10666-007-9106-6>.
- Environment Agency, 2008. Review of Modelling Methods of Near-Field Acid Deposition. European Commission, 2012. The multifunctionality of green infrastructure. DG Environ. Brussels.
- Godłowska, J., Kaszowski, W., 2019. Testing various morphometric methods for determining the vertical profile of wind speed above Krakow, Poland. *Boundary-Layer Meteorol.* 172, 107–132. <https://doi.org/10.1007/s10546-019-00440-9>.
- Goodsite, M.E., Hertel, O., Johnson, M.S., Jørgensen, N.R., 2021. Urban air quality: sources and concentrations. In: Goodsite, M.E., Johnson, M.S., Hertel, O. (Eds.), *Air Pollution Sources, Statistics and Health Effects*. Springer US, New York, NY, pp. 193–214. https://doi.org/10.1007/978-1-0716-0596-7_321.
- Gromke, C., Buccolieri, R., Di Sabatino, S., Ruck, B., 2008. Dispersion study in a street canyon with tree planting by means of wind tunnel and numerical investigations - evaluation of CFD data with experimental data. *Atmos. Environ.* 42, 8640–8650. <https://doi.org/10.1016/j.atmosenv.2008.08.019>.
- Gromke, C., Jamarkattel, N., Ruck, B., 2016. Influence of roadside hedgerows on air quality in urban street canyons. *Atmos. Environ.* 139, 75–86. <https://doi.org/10.1016/j.atmosenv.2016.05.014>.
- Gromke, C., Ruck, B., 2009. On the impact of trees on dispersion processes of traffic emissions in street canyons. *Boundary-Layer Meteorol.* 131, 19–34. <https://doi.org/10.1007/s10546-008-9301-2>.
- Gromke, C., Ruck, B., 2008. Aerodynamic modelling of trees for small-scale wind tunnel studies. *Forestry* 81, 243–258. <https://doi.org/10.1093/forestry/cpn027>.
- Gromke, C., Ruck, B., 2007. Influence of trees on the dispersion of pollutants in an urban street canyon-Experimental investigation of the flow and concentration field. *Atmos. Environ.* 41, 3287–3302. <https://doi.org/10.1016/j.atmosenv.2006.12.043>.
- Hamada, S., Ohta, T., 2010. Seasonal variations in the cooling effect of urban green areas on surrounding urban areas. *Urban For. Urban Green.* 9, 15–24. <https://doi.org/10.1016/j.ufug.2009.10.002>.

- Hogstrom, U., 1996. Review of some basic characteristics of the atmospheric surface layer. *Boundary-Layer Meteorol.* 78, 215–246. <https://doi.org/10.1007/BF00120937>.
- Hunt, J.C.R., 1985. Turbulent diffusion from sources in complex flows. *Annu. Rev. Fluid Mech.* 17, 447–485.
- Hunt, J.C.R., Leibovich, S., Richards, K.J., 1988a. Turbulent shear flows over low hills. *Q. J. R. Meteorol. Soc.* 114, 1435–1470. <https://doi.org/10.1002/qj.49711448405>.
- Hunt, J.C.R., Richards, K.J., Brighton, P.W.M., 1988b. Stably stratified shear flow over low hills. *Q. J. R. Meteorol. Soc.* 114, 859–886. <https://doi.org/10.1002/qj.49711448203>.
- Janhäll, S., 2015. Review on urban vegetation and particle air pollution - deposition and dispersion. *Atmos. Environ.* 105, 130–137. <https://doi.org/10.1016/j.atmosenv.2015.01.052>.
- Jeanjean, A., Buccolieri, R., Eddy, J., Monks, P., Leigh, R., 2017. Air quality affected by trees in real street canyons: the case of Marylebone neighbourhood in central London. *Urban For. Urban Green.* 22, 41–53. <https://doi.org/10.1016/j.ufug.2017.01.009>.
- Jeanjean, A.P.R., Hinchliffe, G., McMullan, W.A., Monks, P.S., Leigh, R.J., 2015. A CFD study on the effectiveness of trees to disperse road traffic emissions at a city scale. *Atmos. Environ.* 120, 1–14. <https://doi.org/10.1016/j.atmosenv.2015.08.003>.
- Jeanjean, A.P.R., Monks, P.S., Leigh, R.J., 2016. Modelling the effectiveness of urban trees and grass on PM2.5 reduction via dispersion and deposition at a city scale. *Atmos. Environ.* 147, 1–10. <https://doi.org/10.1016/j.atmosenv.2016.09.033>.
- Kent, C.W., Grimmond, S., Barlow, J., Gatey, D., Kotthaus, S., Lindberg, F., Halios, C.H., 2017a. Evaluation of urban local-scale Aerodynamic parameters: implications for the vertical profile of wind speed and for source areas. *Boundary-Layer Meteorol.* 164, 1–31. <https://doi.org/10.1007/s10546-017-0248-z>.
- Kent, C.W., Grimmond, S., Gatey, D., 2017b. Aerodynamic roughness parameters in cities: inclusion of vegetation. *J. Wind Eng. Ind. Aerod.* 169, 168–176. <https://doi.org/10.1016/j.jweia.2017.07.016>.
- Kong, F., Yin, H., James, P., Hutyrá, L.R., He, H.S., 2014. Effects of spatial pattern of greenspace on urban cooling in a large metropolitan area of eastern China. *Landsc. Urban Plann.* 128, 35–47. <https://doi.org/10.1016/j.landurbplan.2014.04.018>.
- Kong, F., Yin, H., Nakagoshi, N., Zong, Y., 2010. Urban green space network development for biodiversity conservation: identification based on graph theory and gravity modeling. *Landsc. Urban Plann.* 95, 16–27. <https://doi.org/10.1016/j.landurbplan.2009.11.001>.
- Leo, L.S., Buccolieri, R., Di Sabatino, S., 2018. Scale-adaptive morphometric analysis for urban air quality and ventilation applications. *Build. Res. Inf.* 46, 931–951. <https://doi.org/10.1080/09613218.2018.1501797>.
- Li, X.B., Lu, Q.C., Lu, S.J., He, H. Di, Peng, Z.R., Gao, Y., Wang, Z.Y., 2016. The impacts of roadside vegetation barriers on the dispersion of gaseous traffic pollution in urban street canyons. *Urban For. Urban Green.* 17, 80–91. <https://doi.org/10.1016/j.ufug.2016.03.006>.
- Macdonald, R.W., 2000. Modelling the mean velocity profile in the urban canopy layer. *Boundary-Layer Meteorol.* 97, 25–45. <https://doi.org/10.1023/A:1002785830512>.
- MacDonald, R.W., Griffiths, R.F., Hall, D.J., 1998. An improved method for the estimation of surface roughness of obstacle arrays. *Atmos. Environ.* 32, 1857–1864.
- McDonald, R.L., 2015. *Conservation for Cities: How to Plan & Build Natural Infrastructure*. Island Press.
- Nowak, D.J., Crane, D.E., Stevens, J.C., 2006. Air pollution removal by urban trees and shrubs in the United States. *Urban for. Urban Green* 4, 115–123. <https://doi.org/10.1016/j.ufug.2006.01.007>.
- Pernigotti, D., Georgieva, E., Thunis, P., Bessagnet, B., 2012. Impact of meteorology on air quality modeling over the Po valley in northern Italy. *Atmos. Environ.* 51, 303–310. <https://doi.org/10.1016/j.atmosenv.2011.12.059>.
- Piringer, M., Petz, E., Groehn, I., Schaubberger, G., 2007. A sensitivity study of separation distances calculated with the Austrian Odour Dispersion Model (AODM). *Atmos. Environ.* 41, 1725–1735. <https://doi.org/10.1016/j.atmosenv.2006.10.028>.
- Raffaelli, K., Deserti, M., Stortini, M., Amorati, R., Vasconi, M., Giovannini, G., 2020. Improving air quality in the Po valley, Italy: some results by the LIFE-IP-PREPAIR project. *Atmosphere (Basel)* 11. <https://doi.org/10.3390/ATMOS11040429>.
- Ratti, C., Di Sabatino, S., Britter, R., 2006. Urban texture analysis with image processing techniques: winds and dispersion. *Theor. Appl. Climatol.* 84, 77–90. <https://doi.org/10.1007/s00704-005-0146-z>.
- Redon, E., Lemonsu, A., Masson, V., 2020. An urban trees parameterization for modeling microclimatic variables and thermal comfort conditions at street level with the Town Energy Balance model (TEB-SURFEX v8.0). *Geosci. Model Dev. (GMD)* 13, 385–399. <https://doi.org/10.5194/gmd-13-385-2020>.
- Ries, K., Eichhorn, J., 2001. Simulation of effects of vegetation on the dispersion of pollutants in street canyons. *Meteorol. Z.* 10, 229–233. <https://doi.org/10.1127/0941-2948/2001/0010-0229>.
- Salmond, J.A., Tadaki, M., Vardoulakis, S., Arbuthnott, K., Coutts, A., Demuzere, M., Dirks, K.N., Heaviside, C., Lim, S., MacIntyre, H., McInnes, R.N., Wheeler, B.W., 2016. Health and climate related ecosystem services provided by street trees in the urban environment. *Environ. Heal. A Glob. Access Sci. Source* 15. <https://doi.org/10.1186/s12940-016-0103-6>.
- Santiago, J.L., Martilli, A., Martin, F., 2017. On dry deposition modelling of atmospheric pollutants on vegetation at the microscale: application to the impact of street vegetation on air quality. *Boundary-Layer Meteorol.* 162, 451–474. <https://doi.org/10.1007/s10546-016-0210-5>.
- Selmi, W., Weber, C., Rivière, E., Blond, N., Mehdi, L., Nowak, D., 2016. Air pollution removal by trees in public green spaces in Strasbourg city, France. *Urban For. Urban Green.* 17, 192–201. <https://doi.org/10.1016/j.ufug.2016.04.010>.
- Song, X.P., Tan, P.Y., Edwards, P., Richards, D., 2018. The economic benefits and costs of trees in urban forest stewardship: a systematic review. *Urban For. Urban Green.* 29, 162–170. <https://doi.org/10.1016/j.ufug.2017.11.017>.
- Soulhac, L., Salizzoni, P., Cierco, F.X., Perkins, R., 2011. The model SIRANE for atmospheric urban pollutant dispersion; part I, presentation of the model. *Atmos. Environ.* 45, 7379–7395. <https://doi.org/10.1016/j.atmosenv.2011.07.008>.
- Stocker, J., Hood, C., Carruthers, D., McHugh, C., 2012. ADMS-Urban: developments in modelling dispersion from the city scale to the local scale. *Int. J. Environ. Pollut.* 50, 308–316.
- Tallis, M., Taylor, G., Sinnett, D., Freer-Smith, P., 2011. Estimating the removal of atmospheric particulate pollution by the urban tree canopy of London, under current and future environments. *Landsc. Urban Plann.* 103, 129–138. <https://doi.org/10.1016/j.landurbplan.2011.07.003>.
- Thunis, P., Triacchini, G., White, L., Maffei, G., Volta, M., 2009. Air pollution and emission reductions over the Po-valley: air quality modelling and integrated assessment. 18th World IMACS Congr. MODSIM 2009 - Int. Congr. Model. Simul. Interfacing Model. Simul. with Math. Comput. Sci. Proc. 2335–2341.
- Tiwari, A., Kumar, P., 2020. Integrated dispersion-deposition modelling for air pollutant reduction via green infrastructure at an urban scale. *Sci. Total Environ.* 723, 138078. <https://doi.org/10.1016/j.scitotenv.2020.138078>.
- Tiwari, A., Kumar, P., Baldauf, R., Zhang, K.M., Pilla, F., Di Sabatino, S., Brattich, E., Pulvirenti, B., 2019. Considerations for evaluating green infrastructure impacts in microscale and macroscale air pollution dispersion models. *Sci. Total Environ.* 672, 410–426. <https://doi.org/10.1016/j.scitotenv.2019.03.350>.
- Tositti, L., Brattich, E., Masiol, M., Baldacci, D., Ceccato, D., Parmeggiani, S., Stracquadanio, M., Zappoli, S., 2014. Source apportionment of particulate matter in a large city of southeastern Po Valley (Bologna, Italy). *Environ. Sci. Pollut. Res.* 21, 872–890. <https://doi.org/10.1007/s11356-013-1911-7>.
- Tzoulas, K., Korpela, K., Venn, S., Yli-Pelkonen, V., Kaźmierczak, A., Niemela, J., James, P., 2007. Promoting ecosystem and human health in urban areas using Green Infrastructure: a literature review. *Landsc. Urban Plann.* 81, 167–178. <https://doi.org/10.1016/j.landurbplan.2007.02.001>.
- Vos, P.E.J., Maiheu, B., Vankerkom, J., Janssen, S., 2013. Improving local air quality in cities: to tree or not to tree? *Environ. Pollut.* 183, 113–122. <https://doi.org/10.1016/j.envpol.2012.10.021>.
- Vranckx, S., Vos, P., Maiheu, B., Janssen, S., 2015. Impact of trees on pollutant dispersion in street canyons: a numerical study of the annual average effects in Antwerp, Belgium. *Sci. Total Environ.* 532, 474–483. <https://doi.org/10.1016/j.scitotenv.2015.06.032>.
- Wania, A., Bruse, M., Blond, N., Weber, C., 2012. Analysing the influence of different street vegetation on traffic-induced particle dispersion using microscale simulations. *J. Environ. Manag.* 94, 91–101. <https://doi.org/10.1016/j.jenvman.2011.06.036>.
- Wolf, K.L., 2003. Ergonomics of the city : green infrastructure and social benefits. In: *Eng. Green Proc. 2003 Natl. Urban for. Conf.* 2003, p. 5.
- Yuan, C., Norford, L., Ng, E., 2017. A semi-empirical model for the effect of trees on the urban wind environment. *Landsc. Urban Plann.* 168, 84–93. <https://doi.org/10.1016/j.landurbplan.2017.09.029>.